

**PALM OIL BASED ALKYD/POLYANILINE AS
ELECTRICALLY CONDUCTIVE COATING WITH UV
CURING ABILITY**

SITI NUR AMALINA BINTI RAMLAN

**FACULTY OF SCIENCE
UNIVERSITY OF MALAYA
KUALA LUMPUR**

2018

**PALM OIL BASED ALKYD/POLYANILINE AS
ELECTRICALLY CONDUCTIVE COATING WITH UV
CURING ABILITY**

SITI NUR AMALINA BINTI RAMLAN

**DISSERTATION SUBMITTED IN FULFILMENT OF
THE REQUIREMENTS FOR THE DEGREE OF MASTER
OF SCIENCE (EXCEPT MATHEMATICS & SCIENCE
PHILOSOPHY)**

**DEPARTMENT OF CHEMISTRY
FACULTY OF SCIENCE
UNIVERSITY OF MALAYA
KUALA LUMPUR**

2018

UNIVERSITY OF MALAYA
ORIGINAL LITERARY WORK DECLARATION

Name of Candidate: Siti Nur Amalina binti Ramlan

Matric No: SGR150002

Name of Degree: Master of Science (except Mathematics & Science Philosophy)

Title of Project Paper/Research Report/Dissertation/Thesis (“this Work”): Palm Oil Based Alkyd/Polyaniline as Electrically Conductive Coating with UV Curing Ability

Field of Study: Polymer Chemistry

I do solemnly and sincerely declare that:

- (1) I am the sole author/writer of this Work;
- (2) This Work is original;
- (3) Any use of any work in which copyright exists was done by way of fair dealing and for permitted purposes and any excerpt or extract from, or reference to or reproduction of any copyright work has been disclosed expressly and sufficiently and the title of the Work and its authorship have been acknowledged in this Work;
- (4) I do not have any actual knowledge nor do I ought reasonably to know that the making of this work constitutes an infringement of any copyright work;
- (5) I hereby assign all and every rights in the copyright to this Work to the University of Malaya (“UM”), who henceforth shall be owner of the copyright in this Work and that any reproduction or use in any form or by any means whatsoever is prohibited without the written consent of UM having been first had and obtained;
- (6) I am fully aware that if in the course of making this Work I have infringed any copyright whether intentionally or otherwise, I may be subject to legal action or any other action as may be determined by UM.

Candidate’s Signature

Date:

Subscribed and solemnly declared before,

Witness’s Signature

Date:

Name:

Designation:

PALM OIL BASED ALKYD/POLYANILINE AS ELECTRICALLY CONDUCTIVE COATING WITH UV CURING ABILITY

ABSTRACT

Environmentally friendly products are gaining popularity recently, in line with the increasing global demand for green technology. Ultraviolet (UV)-curable coating is one of them since it involves minimal, if any, emission of volatile organic compounds during the curing process. Besides, UV curing technology enables coatings to be cured within much shorter time compared to thermal curing process. The aim of this study is to produce electrically conductive UV-curable coating which is environmentally friendly. Polyaniline is a polymer with excellent electrical conductivity and it is known to exhibit anti-corrosion properties through passivation. However, polyaniline itself is not a good coating binder, as it tends to produce brittle film with poor adhesion. Therefore, in this work palm oil-based polyester binder was synthesized and blended with polyaniline to produce electrically active coating with improved film properties. The alkyd resin was formulated with considerable amount of maleic acid formulation in order to render it UV-curable. Both alkyd and polyaniline was characterized using FTIR, ¹H-NMR, TGA and UV-Vis. Some of the tests carried out to investigate the film properties of the coatings include pencil hardness test, adhesion tape test, water and chemical resistant test, conductivity, and thermal stability. Alkyd has improved poor coating binder properties of polyaniline in term of their mechanical properties. In addition, anticorrosion property of the coatings on mild steels were determined using open circuit potential (OCP) values, Tafel analysis and electrochemical impedance spectroscopy (EIS). Alkyd coating which contains 0.5% polyaniline shows improved corrosion resistance properties with corrosion rate 2.277×10^{-5} mm/y. A stable and homogeneous alkyd/polyaniline coating film has been prepared in this project with

evidences from the FTIR analyses and conductivity studies showing strong interaction between alkyd and polyaniline through crosslinking reaction.

Keywords: UV-curable coating, palm oil-based binder, polyaniline, conductivity, anti-corrosion

**ALKID/POLIANILIN BERASASKAN MINYAK KELAPA SAWIT SEBAGAI
SALUTAN KONDUKTIF ELEKTRIK DENGAN KEBOLEHAN UV SILANG KAIT**

ABSTRAK

Produk mesra alam semakin popular baru-baru ini, sejajar dengan permintaan global teknologi hijau yang semakin meningkat. Salutan yang disilang kait oleh sinaran ultraungu (UV) adalah salah satu produk tersebut kerana jumlah pelepasan sebatian organik yang meruap semasa proses silang kait ini adalah sangat minima. Di samping itu, teknologi silang kait oleh UV membolehkan salutan disilang kait dalam masa yang singkat berbanding proses silang kait menggunakan haba. Tujuan kajian ini adalah untuk menghasilkan salutan mesra alam yang mampu disilang kait oleh UV dan bersifat konduktif. Polianilin adalah polimer yang mempunyai kekonduksian elektrik yang sangat baik dan terkenal sebagai agen anti-karat melalui proses ‘passivation’. Walau bagaimanapun, polianilin sahaja tidak boleh menjadi salutan yang boleh melekat dengan baik, ia cenderung untuk menghasilkan lapisan yang rapuh oleh kerana sifat lekatan yang lemah. Oleh itu, dalam kajian ini, poliester berasaskan minyak kelapa sawit telah disintesis sebagai pelekat dan digabungkan dengan polyanilin untuk menghasilkan salutan yang membolehkan elektrik mengalir dengan baik serta mempunyai sifat lekatan yang kuat. Resin alkid diformulasikan dengan pertambahan asid maleik untuk membolehkan ia disilang kait dengan teknologi UV. Kedua-dua alkid dan polianilin dicirikan menggunakan FTIR, ¹H-NMR, TGA dan UV-Vis. Beberapa ujian dijalankan untuk menyiasat sifat-sifat lapisan antaranya ujian kekerasan pensil, ujian pita lekat, ujian ketahanan terhadap air dan larutan kimia, kekonduksian dan kestabilan terma. Alkid telah memperbaiki sifat pengikat salutan polianilin yang lemah dari segi sifat mekanikalnya. Di samping itu, ujian kekaratan salutan di atas keluli ditentukan menggunakan nilai litar terbuka berpotensi (OCP), analisis Tafel dan elektrokimia impedans spektroskopi (EIS). Salutan alkid yang mengandungi 0.5% polyanilin

memperlihatkan ciri rintangan kekaratan yang lebih baik dengan kadar karat 2.277×10^{-5} mm/y. Lapisan salutan alkid/polyanilin yang stabil dan homogen telah disediakan dalam projek ini berdasarkan bukti daripada analisis FTIR dan kajian kekonduksian yang menunjukkan interaksi kuat antara alkid dan polyanilin melalui tindak balas silang kait.

Kata kunci: Salutan silang kait UV, salutan berasaskan minyak kelapa sawit, polianilin, konduktiviti, anti-karat

ACKNOWLEDGEMENTS

First of all, I would like to take this opportunity to express a deep sense of gratitude to my supervisor, Dr Desmond Ang Teck Chye for his valuable guidance and supports throughout this project. Not forgetting my co-supervisors Prof Wan Jeffrey Basirun and Dr Phang Sook Wai for their kind association as well as supervision in this research study. Many thanks to all my friends and staff of the Chemistry Department University of Malaya for their help in many ways. I also would like to thank Dr. Kavirajaa Pandian Sambasevam and Magaji Ladan (BUK) for their guidance in coatings characterization and EIS measurement. Special thanks to my lovely husband, Muhammad Taufiq bin Zaini, all family members especially my parents, Ramlan bin Ibrahim and Rozita binti Zakaria for their encouragements and supports throughout my study. Last but not least, I would like to thank the source of the financial support for this project by Ministry of Science and Technology Malaysia, MOSTI (SF006-2015), and Ministry of Higher Education (MOHE) for the scholarships.

TABLE OF CONTENTS

Abstract.....	iii
Abstrak.....	v
Acknowledgements.....	vii
Table of contents.....	viii
List of figures.....	xii
List of tables.....	xiv
List of symbols and abbreviations	xv
List of appendices	xvii
CHAPTER 1: INTRODUCTION.....	1
1.1 Background of study	1
1.2 Objectives of the research	5
1.3 Scopes of study.....	5
1.4 Outline of the dissertation	6
CHAPTER 2: LITERATURE REVIEW	7
2.1 Alkyd	7
2.1.1 Uses and limitation.....	7
2.1.2 Worldwide consumption	9
2.1.3 Alkyd modification	11
2.1.4 Applications	12
2.2 Conducting Polymer.....	15
2.3 Alkyd/PANI coating.....	17
2.4 UV-curable coating	20
2.4.1 Background	20

2.4.2	Mechanism of curing	21
2.4.3	Advantages	23
2.4.4	Applications	25
2.5	Corrosion and anti-corrosive coating	27
2.5.1	Components in anticorrosive coating.....	29
2.5.2	Protective mechanism	29
2.6	Conductive coating.....	32
CHAPTER 3: METHODOLOGY		34
3.1	Materials.....	34
3.2	Characterizations of palm olein.....	34
3.2.1	Fourier transform infrared spectroscopy (FTIR).....	34
3.2.2	Proton nuclear magnetic resonance spectroscopy (¹ H-NMR).....	34
3.3	Synthesis of alkyd	35
3.4	Characterizations of alkyd.....	36
3.4.1	Determination of acid number.....	36
3.4.2	FTIR spectroscopy	37
3.4.3	¹ H-NMR spectroscopy	37
3.4.4	Thermal analysis	37
3.5	Characterizations of polyaniline (PANI).....	37
3.5.1	FTIR spectroscopy	37
3.5.2	Ultraviolet-visible spectroscopy.....	37
3.5.3	Conductivity test	38
3.5.4	Thermal analysis	38
3.6	Preparation of alkyd/PANI coating	38
3.6.1	Preparation of coating mixture.....	38
3.6.2	Treatment of mild steel	39

3.6.3	Application and curing of coatings	39
3.7	Film properties of cured coatings	41
3.7.1	Pencil hardness test (PHT): ASTM D3363 - 00.....	41
3.7.2	Crosshatch adhesion tape test: ASTM D3359 - 97	42
3.7.3	Water and alkali resistance test: ASTM D1647 - 89.....	43
3.7.4	Acid resistance and salt water resistance tests	44
3.7.5	Ultraviolet-visible spectroscopy.....	44
3.7.6	Thermal Analysis	44
3.8	Development of UV-curable alkyd/PANI coating	44
3.8.1	Effect of coating composition (Alkyd:PANI) on film conductivity	44
3.8.2	Effect of UV curing time on film conductivity and FTIR analyses	45
3.9	Surface study and electrochemical methods.....	45
CHAPTER 4: RESULTS AND DISCUSSIONS		48
4.1	Characterizations of palm olein.....	48
4.1.1	FTIR spectroscopy	48
4.1.2	¹ H-NMR spectroscopy	50
4.2	Characterizations of alkyd.....	52
4.2.1	Determination of acid number.....	52
4.2.2	FTIR spectroscopy	52
4.2.3	¹ H-NMR spectroscopy	54
4.2.4	Thermal analysis	57
4.3	Characterizations of PANI	58
4.3.1	FTIR spectroscopy	58
4.3.2	UV-Vis spectroscopy	60
4.3.3	Thermal analysis	61
4.4	Alkyd/PANI Film Properties.....	62

4.4.1	Effect of coating composition (Alkyd:PANI) on film conductivity	62
4.4.2	UV-Vis spectroscopy	63
4.4.3	Film properties	64
4.4.4	Thermal Analysis	66
4.4.5	Effect of UV curing time on film conductivity and FTIR analyses	67
4.5	Surface and electrochemical study	70
4.5.1	Field-emission scanning electron microscopy analysis (FESEM).....	70
4.5.2	Open circuit potentials analysis	70
4.5.3	EIS analysis	71
4.5.4	Tafel polarization measurements	74
 CHAPTER 5: CONCLUSIONS AND SUGGESTION FOR FURTHER RESEARCH		77
5.1	Conclusions	77
5.2	Suggestion for further research	78
	References.....	79
	List of Publications and Papers Presented	89
	Appendix	91

LIST OF FIGURES

Figure 1.1	: Formation of polyester glyptal	1
Figure 1.2	: Different oxidation states of polyaniline	4
Figure 2.1	: World consumption of alkyd surface coatings in 2016	9
Figure 2.2	: Examples of conducting polymer	16
Figure 2.3	: Schematic of the bead mill with centrifugal bead separation	19
Figure 2.4	: Basic mechanism for free-radical photocurable system	22
Figure 2.5	: Curing mechanisms of (a) physically drying coating and (b) chemically curing coating	24
Figure 2.6	: Thermograms of (a) UV-curable tung oil (UVTO) formula and (b) UV-curable tung-based alkyd (UVTA) formula	27
Figure 2.7	: Economic loss from corrosion of materials in Beijing	28
Figure 2.8	: Schematic diagram of mechanism of passivation by PANI on steel	31
Figure 2.9	: Protective mechanisms of anticorrosive coatings	32
Figure 3.1	: Experimental set-up for (a) First stage of alkyd cooking; transesterification, and (b) Second stage of alkyd cooking; polycondensation	36
Figure 3.2	: UV curing machine	40
Figure 3.3	: TQC pencil hardness test instrument	41
Figure 3.4	: Pencil hardness scale	41
Figure 3.5	: Water and alkali resistance test set-up	43
Figure 3.6	: EIS cells of coated mild steels	46
Figure 3.7	: Set-up of electrochemical evaluation	47
Figure 4.1	: FTIR spectrum of palm olein	49

Figure 4.2	: ^1H -NMR spectrum of palm olein	51
Figure 4.3	: FTIR spectrum of alkyd	53
Figure 4.4	: ^1H -NMR spectrum of alkyd	55
Figure 4.5	: Plausible synthesis route of the maleated alkyd	56
Figure 4.6	: (a) TGA thermogram of alkyd and (b) 1 st TGA derivative curve (%/min against temperature) of alkyd	57
Figure 4.7	: FTIR spectrum of PANI	59
Figure 4.8	: UV-Vis spectrum of PANI	60
Figure 4.9	: TGA thermogram of PANI	61
Figure 4.10	: UV-Vis spectra of alkyd and alkyd/PANI coatings	63
Figure 4.11	: Overlay of FTIR spectra of coating F with different UV curing times; (a) 0s, (b) 30s, (c) 60s, (d) 90s and (e) 120s	69
Figure 4.12	: FESEM images of (a) Coating K and (b) Coating L	70
Figure 4.13	: OCP variations of coated steel K, L and M during 30 days immersion in 3.5% NaCl	71
Figure 4.14	: Nyquist plots of impedance spectra in various immersion times for (a) Coating K, (b) Coating L and (c) Coating M coated on mild steel in 3.5% NaCl solution	73
Figure 4.15	: Nyquist plots of impedance spectra after 25 days immersion of Coating K, L and M coated on mild steel in 3.5% NaCl solution	74
Figure 4.16	: Tafel Plot for coating K (Alkyd), coating L (0.50% PANI) and coating M (1% PANI)	75
Figure 4.17	: Coated mild steels for coating K, L and M before and after immersed in 3.5% NaCl for 30 days	76

LIST OF TABLES

Table 2.1	: Polymers commonly used to modify alkyd resins	11
Table 2.2	: Adhesion properties of PANI/alkyd nanocomposites with different proportions of alkyd	18
Table 2.3	: Basic components of UV-curables	21
Table 3.1	: Compositions of coating mixtures	39
Table 3.2	: Classification of adhesion test results	42
Table 4.1	: Peak assignments for FTIR spectrum of palm olein	48
Table 4.2	: Peak assignments for ^1H -NMR spectrum of palm olein	50
Table 4.3	: Peak assignments for FTIR spectrum of alkyd	53
Table 4.4	: Peak assignments for ^1H -NMR spectrum of alkyd	54
Table 4.5:	: Conductivity of coating mixtures contain different ratios of alkyd and PANI	62
Table 4.6	: UV-Vis absorption peaks assignments for alkyd/PANI coatings	64
Table 4.7	: Physicochemical properties of UV-cured coatings	65
Table 4.8	: E_d of coatings based on Kissinger equation	67
Table 4.9	: Conductivity of coating F with different UV curing times	68
Table 4.10	: Impedance parameters of coatings K, L and M coated on mild steel in 3.5% NaCl solution	72
Table 4.11	: Data from Tafel Plot analysis	75

LIST OF SYMBOLS AND ABBREVIATIONS

$^1\text{H-NMR}$: Proton nuclear magnetic resonance
AFM	: Atomic force spectroscopy
ASTM	: American Society for Testing and Materials
BUK	: Bayero University Kano
CNY	: China Yuan
DSC	: Differential Scanning Calorimetry
DSSC	: Dye-sensitized solar cell
ECG	: Electrocardiography
E_d	: Activation energy of decomposition
EIS	: Electrical impedance spectroscopy
EMI	: Electromagnetic interference
ENM	: Electrochemical noise method
FRA	: Frequency response analyzer
FTIR	: Fourier Transform Infrared
FTO	: Fluorine-doped tin oxide
GMR	: Giant magnetoresistance
ICP	: Intrinsic conducting polymer
IPCE	: Incident photon to current conversion efficiency
k_p	: Rate constant of propagation step
k_t	: Rate constant of termination step
MMA	: Methyl methacrylate
MOHE	: Ministry of Higher Education
MOSTI	: Ministry of Science, Technology and Innovation Malaysia
MPOC	: Malaysian Palm Oil Council

OCP	: Open Circuit Potential
PANI	: Polyaniline
PEDOT	: Poly(3,4-ethylenedioxythiophene)
PHT	: Pencil Hardness Test
PSS	: Poly(styrenesulfonate)
S	: Siemens
SCE	: Saturated calomel electrode
TGA	: Thermal gravimetric analyser
TMPTA	: Trimethylolpropane triacrylate
TMS	: Tetramethylsilane
TPGDA	: Tripropylene glycol diacrylate
UV	: Ultraviolet
UV-Vis	: Ultraviolet-visible
UVTA	: UV-curable tung-based alkyd
UVTO	: UV-curable tung oil
VOCs	: Volatile organic compounds

LIST OF APPENDICES

Appendix: Derivative TGA thermograms of UV-cured coatings at different heating rates	91
---	----

CHAPTER 1: INTRODUCTION

1.1 Background of study

Nowadays, conventional conductive coatings are prepared with metal content in the products and provide good anticorrosive property. However, a common problem associated with the use of metal in conductive coating is the tendency of the metal to undergo oxidation and sedimentation. Therefore, the main objective of this study is to prepare a coating using palm oil-based alkyd as the resins, blended with conducting polymer in order to derive the electrical conductivity of the coating. In this study, alkyd is synthesized using mixture of palm oil, glycerol and diacids (phthalic anhydride and maleic acid). Alkyd resins were first synthesized in the 1920s then came into commercial use over 50 years ago and known as one of the most important types of surface coating. The name alkyd, formed from alkyl (alcohol) and acid, denotes the chemical origin of the resin, which is commonly based on a polymerization reaction between an alcohol, such as glycerol, and a dicarboxylic acid or its anhydride. Glycerol and phthalic anhydride react to form the polyester glyptal. The reaction can be represented as follows:

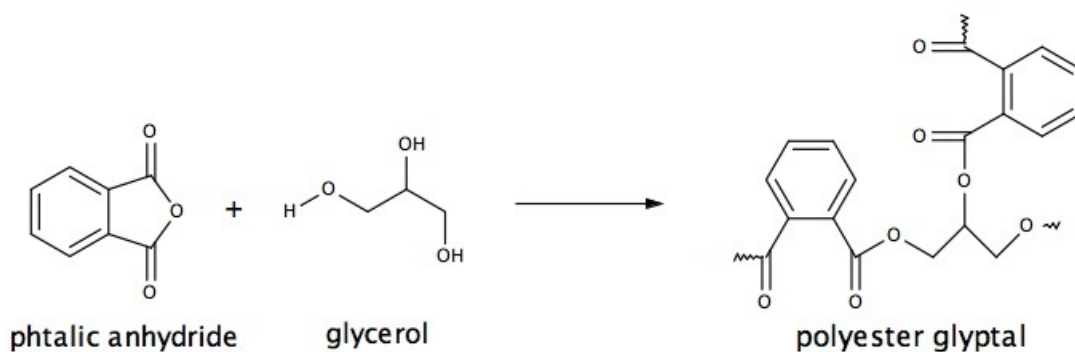


Figure 1.1: Formation of polyester glyptal

A branched polyester containing fatty-acid side groups will produce when an unsaturated oil such as palm oil, linseed oil, tung oil, or dehydrated castor oil is added to the ester-forming compounds. When such a coating agent is applied to a surface, the oil portion of the polyester undergoes a cross-linking reaction in the presence of oxygen from the surrounding air and yielding a tack-free film as it dries.

Alkyd resins have been well-defined as the reaction product of a polybasic acid and a polyhydric alcohol. The detailed definition that has gained wide recognition is that alkyds are polyesters modified with monobasic fatty acids. In recent years, the term nonoil or oil-free alkyd has come into use to describe polyesters formed by the reaction of polybasic acids with polyhydric alcohols in non-stoichiometric amounts. These products are founded rapidly increasing uses in organic coatings and best described as functional saturated polyesters containing unreacted OH and/or COOH groups. Alkyd resins still ranked as the most important synthetic coating resins while constitute about 35% of all resins and even with the wide array of other polymers for coatings that have introduced in more recent years (Lanson, 1985).

Polyaniline (PANI) is chosen as the conducting polymer in this work because of the ease of synthesis, low cost monomer, good electrochemical properties, tunable properties and better stability at room temperature compared to another conducting polymer. Polyaniline (PANI) is one of the intrinsic conducting polymer (ICP) that have great potential in electrical and electronic industrial applications. PANI is the most stable conducting polymer and widely studied in research area (Coltevieille et al., 1999). PANI may contain either benzenoid, quinoid, or both at different proportions in its molecular structure. PANI can be synthesize by two methods; with or without oxidant but the oxidative chemical synthesis is the most explored. (Visakh et al., 2017). The choices of method to synthesis PANI are depends on the applications of PANI

itself. The chemical methods synthesis of PANI are suitable for producing bulk quantities while the electrochemical methods may be more suitable for controlling particle dimension (Kinyanjui et al., 2006).

PANI is unique since it has different colors, stabilities, and conductivities. Figure 1.2 shows the different oxidation states that PANI can exist. Leucoemeraldine is a colorless substance contains only benzene and amino groups. It is not electrically conducting and oxidizes slowly in air. It may be oxidized in an acidic medium to the green protonated pernigraniline or known as conducting emeraldine salt (*p* doping). Pernigraniline is comprised of alternating aminobenzene and quinonediimine groups. Its salts readily decompose in air since the quinonediimine group is unstable in the presence of nucleophiles which was specifically water. Next, the protonation of the emeraldine base with organic and inorganic acids can produce emeraldine salt of PANI. When emeraldine base of PANI is treated with acids, protons primarily interact with the imine atoms of nitrogen and produce polycations. The total energy of the polymer system increases when the positive charges are localized on neighboring nitrogen atoms while electron density tends to undergo redistribution. Here, the electron pair of nitrogen atoms were unpaired without any change in the amounts of electrons in the system. In a chain, delocalization of cation radicals over a certain conjugation length would provide the electron conductivity of the polymer. This process is named as doping (Boeva & Sergeyev, 2014; Kalendová et al., 2015).

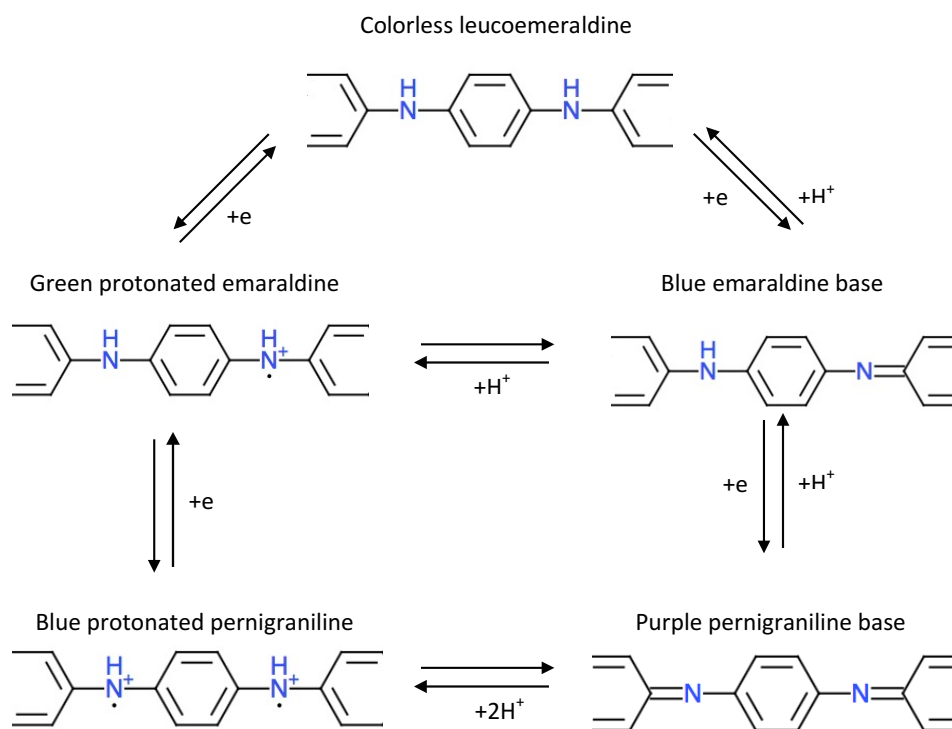


Figure 1.2: Different oxidation states of polyaniline

(Adopted from: Kalendová, A., Veselý, D., Kohl, M., & Stejskal, J. (2015). Anticorrosion efficiency of zinc-filled epoxy coatings containing conducting polymers and pigments. *Progress in Organic Coatings*, 78(Supplement C), 1-20)

The alkyd/PANI composite coating is expected to be economical and environmentally friendly. Another objective in this work is to study the possibility of having the electrically conductive coating with UV-curable ability. UV-curable coating is considered as an environment-friendly coating as it does not involve emission of volatile compounds during UV-curing. In order to render the coating to be UV-curable, there is slight adjustment in the formulation of the resin including increasing the unsaturation in the resins and introducing reactive diluents in the formulation. Cured palm oil-based coating containing doped PANI is expected to be electrically active and exhibit good mechanical properties. Moreover, these coatings are also expected to be able to provide protection against corrosion via passivation of PANI.

1.2 Objectives of the research

In this study, three aims are targeted as following:

- (i) To synthesize and characterize unsaturated alkyd for radiation curable purpose using palm oil as the source of fatty acids.
- (ii) To produce electrically conductive alkyd coating by integrating palm oil-based alkyd with PANI.
- (iii) To investigate physical, electrical, and anti-corrosive properties of UV-cured alkyd/polyaniline coatings on steel.

1.3 Scopes of study

The scope of this research was to synthesize alkyd using palm oil as the main raw material, and maleic acid was introduced in the alkyd formulation to increase the amount of C=C and render it UV curable. The integration of unsaturated diacids in alkyd chain was investigated through spectroscopic method such as FTIR and $^1\text{H-NMR}$. PANI is a conducting polymer which is used as the anticorrosive pigments in the coating and was characterized through spectroscopy method such as FTIR, UV-Vis and conductivity measurement. The alkyd/PANI mixtures were casted into films and several tests inclusive of the pencil hardness test, adhesion tape test, water and chemical resistant test, electrical conductivity, and thermal analysis were conducted to evaluate the film properties of the PANI/alkyd coatings. Besides, the effect of different coating composition on film conductivity was studied by manipulating the proportion of PANI in the coatings. In addition, the effect of UV curing time on film conductivity and FTIR analyses was examined. Finally, the corrosion performance of the coating was studied by common electrochemical methods: open circuit potential (OCP), potentiodynamic polarization, and electrochemical impedance spectroscopy (EIS).

1.4 Outline of the dissertation

This dissertation is presented in five chapters. The first chapter brings a brief introduction on background of study, alkyd, conducting polymer, polyaniline, UV-curable coating, anti-corrosive coating, objectives and scopes of this study. In second chapter, literature reviews on topics related to the study are presented. In follow, all the methodologies involved in this research project are discussed in the third chapter. The fourth chapter discusses on the outputs and justifications of the findings. At the end, the conclusions and suggestions for further research are included in fifth chapter.

CHAPTER 2: LITERATURE REVIEW

2.1 Alkyd

2.1.1 Uses and limitation

Alkyd resin is a complex oil-modified polyester that serves as the film-forming agent in some paints and clear coatings. However, they have yielded preeminence to newer polymer systems (water-based latex paints) because of the volatile organic solvents and low durability on exterior surfaces from alkyd resin. Nevertheless, alkyds are still used in low-performance industrial coatings and in interior paints.

A common alkyd paint consists of the oil-modified polyester, hexane or mineral spirits as solvent to assist in application, metal naphthenates as a catalysis in the drying reaction, and pigment to provide color and hide the coated surface. The oil content of the formulation can vary based on the oil length required. A long-oil alkyd contains 60% fatty acid by weight; a medium-oil alkyd contains 40–60% fatty acid; and a short-oil alkyd contains less than 40%. The use of alkyd coatings is declining partly because of regulations restricting the release of volatile organic content into the atmosphere. In order to solve the problem, alkyds may be made water-reducible by the addition of free acid groups to the molecules. In the presence of a base such as ammonia, these groups allow the polymers to be solubilized in water rather than in organic solvents. Usually a co-solvent such as 2-butoxyethanol is necessary to maintain a stable solution, and under these conditions the ester linkages that are the basis of the alkyd polymer chain are vulnerable to breakage by hydrolysis. In this case, specific monomers are often chosen to give the chain hydrolytic stability.

In surface coatings industry, the single name of polyester, indicates a polyester free of natural-oil modifiers. Such polyesters are used extensively in coatings. The polymer can have a linear structure, but it is often branched, and it is usually in a relatively low-molecular-weight form that can be cross-linked to form a high-performance film. In excess of alcohol, the polyester synthesized tends to have hydroxyl end-groups on the molecules, and these molecules can be cross-linked through the hydroxyl groups by reaction with isocyanate, epoxy, and melamine compounds. In excess of organic acid, the polyester will have carboxyl end-groups during polymerization, and these can become sites for cross-linking with epoxy, melamine, and amine groups. Polyesters with free-acid groups attached to their chains would have same properties with alkyd which can be solubilized to a water-reducible form. Over, the hydrolytic stability of the resultant system must be considered (Lotha, 2016).

Alkyds due to their very good performances, have persisted in the endless competition with the growing synthetic-based polymer resins till now. Because of the great compatibility with many polymers and the large number of formulations, alkyds have proven to be superior to other systems in many applications with special demands. This versatility, combined with their biodegradability while employ a significant amount of renewable material, biological and possibly recyclable, makes alkyds very attractive both from the environmental and the economical point of view (Spasojevic et al., 2015). Alkyd resin has huge advantages towards coating industry since it is flexible, tough, adhesive and durable (Patton, 1962).

2.1.2 Worldwide consumption

Despite there are the growing use of other film formers, alkyd surface coatings remain to be one of the most highly consumed types of coatings used in the world. There are a lot of benefits in alkyd resin systems such as low cost, high versatility and long familiarity with users. They can be modified to meet a variety of end-use requirements through the choice and ratio of reactants and/or modifiers. Alkyds are used extensively in product finishes, architectural coatings and special purpose coatings. Alkyd is basically made from fatty acids or oils derived from renewable sources, hence being considered as an environment friendly materials. Alkyds were the first synthetic coatings binder used in commercial preparation, first used in large quantities in the 1930s.

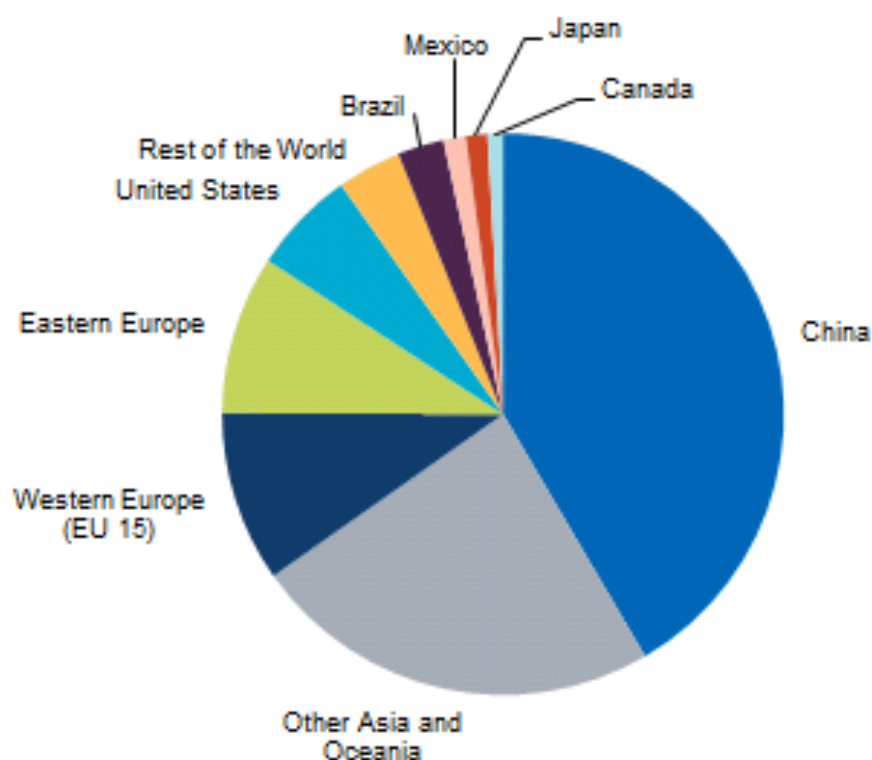


Figure 2.1: World consumption of alkyd surface coatings in 2016

(Source: IHS Markit. (2016). *Chemical Economics Handbook: Alkyd/Polyester Surface Coatings*)

Figure 2.1 shows the pie chart regarding world consumption of alkyd surface coatings according to countries in 2016. In that year, China was the most consumption of alkyd surface coatings. However, consumption of alkyds has diminished over the last 30 years in North America, Western Europe, and Japan. Waterborne emulsions have low odor, low solvent content, easy clean-up, and fast drying properties compared to solventborne alkyds and that was the reasons on the reduction of consumption in the architectural or decorative coatings market. Nevertheless, these emulsions do not display the same degree of performance in leveling, adhesion, gloss, and certain resistance properties in some applications. Therefore, the solventborne alkyds still remain a substantial factor in the coatings industry. However, restrictions on the use of paints are becoming firmer in certain parts of the United States and in Europe, which will forbid the use of conventional low solids solventborne coatings. As a result, the types of resins used in these regions in certain applications will change significantly. There are regulations on restriction of the use of solventborne coatings in many architectural and industrial maintenance coatings applications, especially where there are acceptable latex coatings in the heavily populated regions in California and the northeast United States. In the product finishing market, use of alkyds has declined in recent years because of their replacement with more environmentally acceptable or durable coatings for example powder coatings. Producers continue to develop new and improved systems for high-solids and waterborne formulations to meet increasingly stringent air pollution regulations. In recent years, producers of alkyd resins have developed waterborne latex resins that meet the low VOC levels required by recently enacted legislation in certain parts of the United States and Western Europe (IHS Markit, 2016).

2.1.3 Alkyd modification

Alkyd can be modified by physical or chemical blending with other polymers. Physical mixtures involve simple and straightforward computations compared to chemical modification. Table 2.1 shows polymers that commonly used to modify alkyd resins with different type of modifications (Patton, 1962). Polymer chosen are commonly based on the application for example for basic in appliance and automotive finishes, the combination of alkyds with urea-formaldehyde and melamine-formaldehyde resins are commonly used. Besides, chlorinated products through physical modification of alkyd able to provide heavy-duty coatings for concrete floors and corrosive environment (Patton, 1962). In addition, modification of alkyd with ketone resin also can achieve significant improvements in physical, mechanical, and chemical characteristics of the coatings (Azimi et al., 2013).

Table 2.1: Polymers commonly used to modify alkyd resins

Physical modification	Chemical modification
Nitrocellulose	Styrene
Urea-formaldehyde	Phenolics
Melamine-formaldehyde	Silicones
Chlorinated rubber	Epoxies
Chlorinated paraffin	Isocyanates
	Formaldehyde

2.1.4 Applications

Alkyd is an excellent coating binder as it has good surface coating properties such as high gloss, fast dryness, good corrosion protection and good interactions with polar substrates such as metal, concrete and wood (Cadena et al., 2013; del Amo et al., 1999; Florio & Miller, 2004). Alkyd also widely reported for having good film properties in term of hardness, flexibility, and adhesion to serve as coatings (Aydin et al., 2004; Ang & Gan, 2012). Alkyd has been commonly employed as coating resins owing to its superior properties and is environmentally friendly thus numerous plant oil-based alkyd resin syntheses for coating films have been reported in the literature.

Islam and companion has synthesized three different types of alkyd resins from palm oil by varying the ratios of phthalic and maleic anhydrides. The resulting resins was promising with high gloss and good hardness properties with reasonable drying time around 9 to 12 h in the oven. In this work, they have produced high thermally stable resins that can withstand up to 300°C thus make this resin material suit to act as surface coatings (Islam et al., 2014).

In 2014, another group work on linseed oil based-alkyd resins for paint formulation application. This work involved different amount of oil content in order to utilized linseed oil to obtain alkyd resin. All paint formulations using this alkyd resin have reported to have an excellent film properties since the crosscut experiment shows the achievement of 100% adhesion (İşeri-Çağlar et al., 2014).

However, one of the limitations of alkyd is its weak alkali resistance as reported in the work Ang and Gan. In this work, they used palm stearin as the source of fatty acids for alkyd synthesis. This non-self drying alkyd was modified by incorporating maleic anhydride, MMA and benzophenone as UV photoinitiator to render it UV curable with rapid curing time while produced coatings with good film properties.

Although this alkyd coating is able to exhibit excellent resistance towards water and acid, it showed inferior resistance towards alkali where the alkyd coating in the test showed film depreciation in just under 7 minutes of immersion in NaOH solution (Ang & Gan, 2012). Other researchers also reported the chemical resistance of alkyd film was very strong towards acid, brine and water but vulnerable towards alkali (Aigbodion et al., 2003; Islam et al., 2014). This poor resistance to alkali occurs because ester linkage in the resins are freely attacked by alkalis and hydrolyzed by acid.

Nevertheless, the limitation may be overcome by incorporating additives into the alkyd coating system. Owing to good balance of polar and non-polar moiety in alkyd, it is able to integrate well with wide range of additives. Recent study has been done on modification of alkyd by introduced styrene in the system. Remarkably, this styrenated alkyd resins showed resistance to alkali since the styrenation has prevented the ester linkages of the polyester being damaged from alkali hydrolysis. Besides, the double bonds of styrene present in this styrenated resins improved the adhesion to the substrates (Uzoh et al., 2016).

Besides, alkyd is found to blend well with epoxy resin, reported by Assanvo and colleagues. Results discovered that the blended resins exhibit improved properties which have fast drying time at room temperature, good adhesion, gloss, chemical resistance as well as mechanical properties and has high thermal stability up to 250 °C. From this study, it can be concluded that, the blended of epoxy resins with alkyd synthesized from seeds oil of *R. heudelotii* is a potential renewable candidate for the preparation of fast drying binder and suitable for surface coating applications and industry (Assanvo et al., 2015).

Based on several works, the addition of pigments and nanoparticles into alkyd coatings could enhanced the protective characteristics of the films. In 2001, González

and colleagues found that the resin containing an active pigment such as aluminium powder would have best protection from corrosion on the carbon steel substrate than the base alkyd resin (González et al., 2001). Other works have discovered the addition of extremely small concentration of ZnO nanoparticles (Dhoke et al., 2009) and TiO₂ nanoparticles in alkyd coatings are both effective to improve the corrosion resistance. TiO₂ nanoparticles could inhibit anodic and cathodic reactions on the coating films with high efficiency when there were reductions in the size of TiO₂ nanoparticles and temperature of the system (Deyab & Keera, 2014).

Alkyd coatings have many potential applications in industry. The mechanism of protection of pigmented alkyd coatings are studied by Mills and companions through measurement of the noise resistance, R_n using the electrochemical noise method (ENM). The alkyd coatings perform better than the waterborne coatings by comparing the R_n value from the ENM. Even by visual observation during the time while electrochemical measurements were made, rusting has been observed on the waterborne coatings but not on the alkyd coatings. However, this alkyd paint may be vulnerable to long term exposure to alkali or high chloride solutions since there was a rapid drop in resistance when the solution is changed to concentrated chloride after 200 h. This probably related to the process of ion exchange (Mills et al., 2003).

Alkyds usually produced from non-polluting materials thus known as environmentally friendly coatings. The novel biocompatible palm oil-based alkyds have been synthesized by Teo and colleagues in 2016. These alkyds were confirmed from cell viability assay as non-toxic to 3T3 mouse fibroblasts following exposure of cell cultures for 24 h to solutions of concentration ranging from 3 to 100 µg/mL. These discoveries could recommended this novel bio-sourced alkyds for pharmaceuticals manufacture and controlling drug delivery (Teo et al., 2016).

There are also several works on preparation of alkyd/PANI into coatings (Ecco et al., 2014; Gonçalves et al., 2011; Laco et al., 2005; Martí et al., 2012; Rout et al., 2003). However, most of the coatings reported involves conventional air-drying and thermal curing. In this study, PANI was blended with palm oil-based alkyd to produce electrically active film that cures via UV irradiation. The coatings recorded excellent film properties and was found to exhibit excellent anticorrosion properties.

2.2 Conducting Polymer

Conducting polymers are one of the interested materials studied by a lot of researchers. They have been as an attractive works since they have wide range of electrical conductivity that can be achieved by doping process with high mechanical flexibility and thermal stability properties. These polymers can conduct electricity due to delocalization of Π electrons. Therefore, they may either have metallic conductivity or be semiconductors. Figure 2.2 shows example of conducting polymers. It can be synthesized by numerous methods which include chemical and electrochemical polymerization. Several applications of conducting polymers have been grown up with the improvements of materials stability and control of properties. Organic materials are conducting polymers like insulating polymers. They can achieve high electrical conductivity but the mechanical properties may not be the same as other commercially available polymers. The electrical properties can be adjusted using the methods of organic synthesis and by advanced dispersion techniques. For example, conducting polymers synthesized in the form of nanomaterials are widely investigated because their properties significantly change from the properties of their bulk counterpart. Currently, new technological devices such as electro chromic display devices, photovoltaic devices

and biosensors are developed with these nanostructures of conductive polymers contribution (Awuzie, 2017).

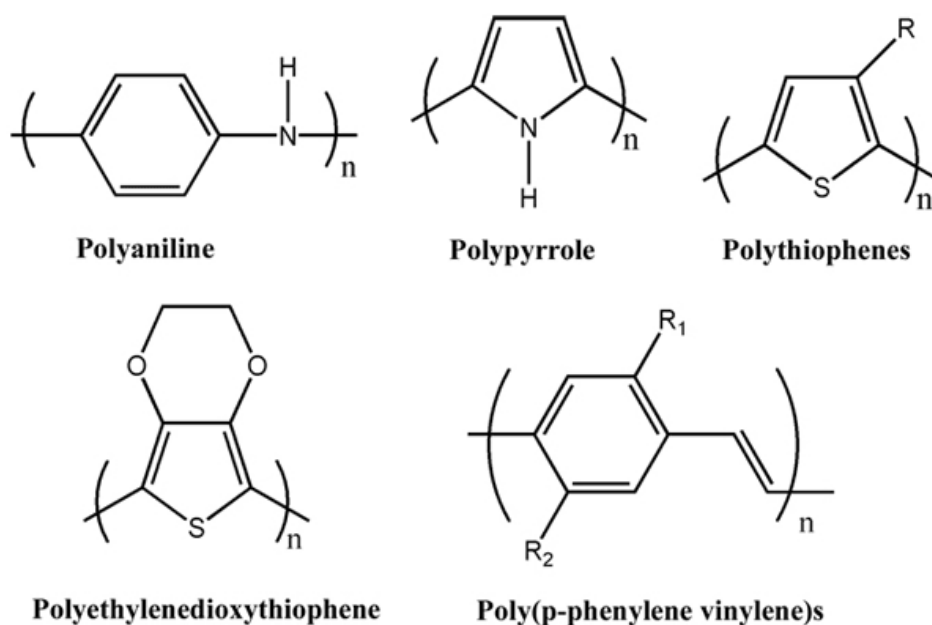


Figure 2.2: Examples of conducting polymer

In coatings area, conducting polymer have superior performance in highly aggressive environments and eco-friendly features thus being extensively investigated for corrosion protection of iron, steel and other metals. In addition, conducting polymer nanocomposites are one of the corrosion protective coatings which were low cost but have better performance and fitted properties. Newly, there are the developments in the corrosion protective performance of conducting polymer composite coatings with natural resource derived polymers. The barrier properties and lifetime of the organic polymeric coatings may improve with the presence of nanoscale dispersion of conducting polymer as filler. These low-cost nanocomposite coatings are expected to play an important role in preventing corrosion which can lead to drastic improvement in corrosion protection (Riaz et al., 2014).

2.3 Alkyd/PANI coating

Conducting polymers however still have their own downsides like poor processability, low yield, low solubility and bad mechanical properties thus restricted their direct applications in various fields, like coatings, optical and solar devices. By then, chemists innovating new methods in their synthesis, where polymers are added to conventional polymers to formulate their copolymer, blends, composites and nanocomposites (Khatoon & Ahmad, 2017).

Polyaniline (PANI) is one of the conducting polymer that was widely studied owing to number of advantages such as ease of synthesis, low cost monomer, good electrochemical properties, unique tunable properties, and it is stable at room temperature (Bhadra et al., 2009; Kalendová et al., 2008). There are many works related to the blends of PANI with other polymers such as polyvinyl chloride, poly(methyl methacrylate) and polystyrene (Bandeira et al., 2017; da Silva et al., 2007; Zhao et al., 2017). Recently, there were also many reported PANI used as fillers to make other conductive polymer nanocomposites (Cheng et al., 2016; Gu et al., 2015; Gu et al., 2013; Guo et al., 2016; Wei et al., 2015; Zhang et al., 2013). However, neat polyaniline is not suitable for coatings purpose due to their poor mechanical properties (Kalendová et al., 2008). That was the reason why they were usually blended with other polymers or introduced as additive into paints or coatings. These blending mixtures render the films electrically active, while maintaining its mechanical strength.

One of the reported systems is alkyd coating containing PANI. Kawata and companions got some problems while using PANI in the counter electrode for dye-sensitized solar cell (DSSC) since the film showed poor adhesion on the FTO glass. Therefore, they have incorporated alkyd into the nanocomposite mixture to improve the

adhesion of the PANI film and the results are shown in Table 2.2. The higher the amount of alkyd in coating mixture, the better the grade obtained from the film adhesion test even before the film is cured. In this work, the strong adhesion of PANI on FTO glass contributed by alkyd as binder has led to higher incident photon to current conversion efficiency (IPCE) in solar cell thus responsible for the stability of the cell (Kawata et al., 2013).

Table 2.2: Adhesion properties of PANI/alkyd nanocomposites with different proportions of alkyd

PANI : alkyd	Film adhesion (uncured coating)	
	Grade	% removal
1:1	5B	0
1:0.75	2B	30
1:0.5	1B	40
1:0.25	0B	100
1:0.1	0B	100

Many studies have been done on this type of coatings but most of them involve conventional method for curing process such as air-drying. Rout and his group have formulated a coating by dispersing PANI powder in a medium oil alkyd resin (binder) with the help of beads mill and showed good dispersibility. Here, the coating was applied on the steel coupons by brush then allowed to dry in the air for atleast 6 h, in order to achieve the optimum drying time for the above coatings formulations (Rout et al., 2003). Figure 2.3 shows the schematic example of the bead mill machine adopted from book written by Wu and Baghdachi that could aid the dispersibility of coating mixture (Wu & Baghdachi, 2015).

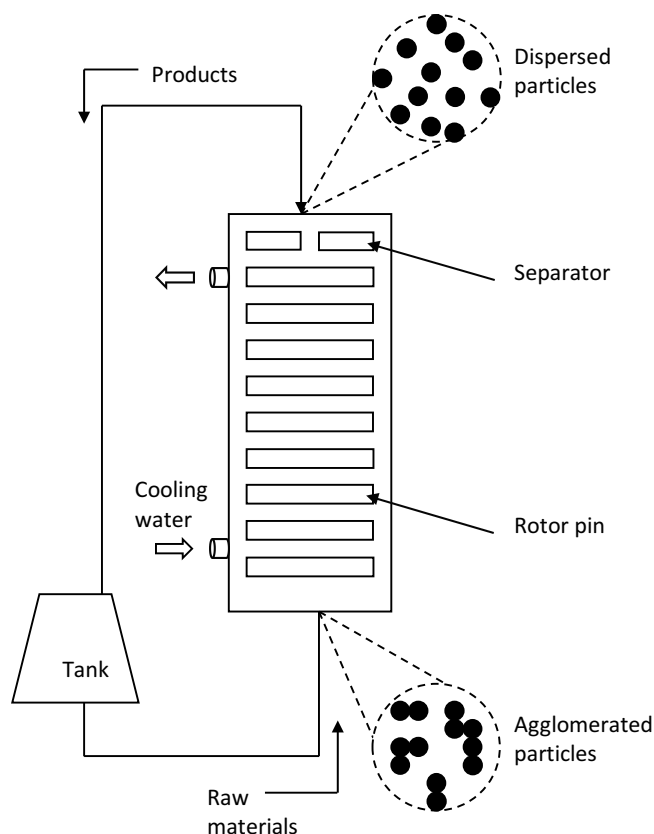


Figure 2.3: Schematic of the bead mill with centrifugal bead separation

(Adopted from: Wu, L., & Baghdachi, J. (2015). *Functional Polymer Coatings: Principles, Methods, and Applications*: Wiley)

Another composite coating prepared by Grgur and colleagues using commercial TESSAROL[®]-Helios, Slovenia, which is a primer for iron based on an alkyd binder and red pigments in organic solvents, modified with 5 wt% PANI-emeraldine salt needs 24 h for drying in the air. This coating mixture was applied using a scalpel-based method on both sides of a clean mild steel (12 cm × 5 cm) sample. They found that incorporating chemically synthesized PANI emeraldine salts could improve the anticorrosion properties of the coating due to their minimal oligomer content. This polyaniline salt was acting as an active barrier protection to prevents the penetration of corrosive agents in the base metals and could last for more than 2 weeks (Grgur et al., 2015).

In 2014, Ecco and his group have studied the anticorrosive properties of an alkyd coating loaded with PANI and cerium oxide (CeO_2) nanoparticles. From salt spray tests, it can be concluded that the influence of this mixture is promising at a certain extent even though the evidences are less professed by means of electrochemical analysis. However, this panels required drying period of 3 weeks at 23 °C – 50% RH plus another week inside a desiccator with dry atmosphere before the beginning of the tests hence can be considered as time-consuming (Ecco et al., 2014).

2.4 UV-curable coating

2.4.1 Background

The ultraviolet (UV) curing technology has attracted industrial interests and started being commercialized in the late 20th century by introducing UV inks product and UV coatings. This UV curing technology has profited various industries. UV curable coatings are said to be environmentally friendly since these systems do not emit volatile organic compounds (VOCs) during the curing process. Paint thinners, air fresheners and aerosol sprays are examples of products with high VOCs contain. VOCs usually released from solvent such as toluene, xylene, styrene and perchloroethylene. These hazardous air pollutants may form ground-level ozone when combined with nitrogen oxides, which contributors to global warming. Besides, exposure to VOCs may lead to loss of coordination, nausea and memory impairment and later can cause damage to the liver, kidneys and the central nervous system (Vickers, 2017). There are four basic components which must be included in order to develop a successful coating in UV curable systems as shown in Table 2.3 (Hoyle, 1990). These photoinitiator, oligomer, monomer, and additive have their own range of percentage and function which make them essential to the UV curable formulation.

Table 2.3: Basic components of UV-curables

Component	Percentage	Function
Photoinitiator	1-3	Free radical or cationic initiation
Oligomer resin	25-90	Film formation and basic properties
Monomers	15-60	Film formation and viscosity control
Additives and fillers	1-50	Surfactants, pigments, stabilizers, etc.
Lamp source	-	Initiate curing

2.4.2 Mechanism of curing

Free-radical chain process is one of the primary types of UV-curable systems. In this system, low molecular weight monomers and oligomers are converted into highly-crosslinked, chemically-resistant films by absorption of UV-radiation. Figure 2.4 shows a simple scheme of mechanism for free-radical photocurable system. Fundamentally, a photoinitiator will absorb light and generates free-radical type initiators or catalysts which convene the crosslinking reactions of functionalized oligomers/monomers to generate a cured film. Firstly, a photoinitiator (PI) absorbs UV-radiation followed by a subsequent reaction to produce a radical initiator ($R\cdot$). According to the traditional mechanism, the radical initiator induces a chain-reaction or chain-growth polymerization (rate constant of the propagation step is k_p) which is terminated, in the absence of oxygen effects, by a radical-radical coupling process (rate constant of termination step is k_t). The rate of the reaction is proportional to the square root of the light intensity (I) and the monomer (M) concentration by assuming steady-state kinetics. Therefore, these two factors; light intensity (I) and the monomer concentration (M) can be adjusted to change the rate of the curing process for a given set of

monomers/oligomers. It can be concluded that the propagation and termination rate constants are dependent on the particular monomers and oligomers employed in the UV-curable formulation and also the photoinitiator used. The efficiency of the generation of $R\cdot$ in the second step as well as the rate constants for chain propagation and termination are the bases for constant 'k' (Hoyle, 1990).

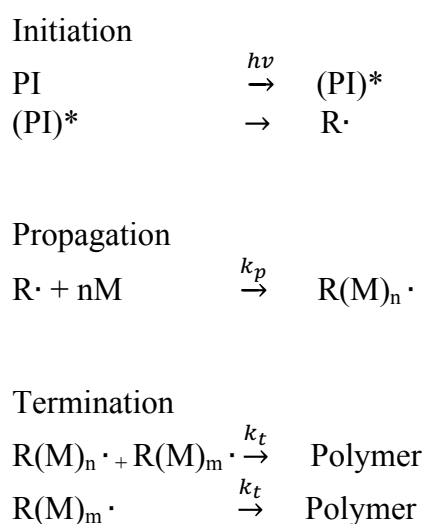


Figure 2.4: Basic mechanism for free-radical photocurable system

Where; PI = photoinitiator

$R\cdot$ = radical initiator

M = monomer

k_p = rate constant of propagation step

k_t = rate constant of termination step

2.4.3 Advantages

One of the unique advantage of UV-curing system is the uses of reactive diluent instead of solvent. This reactive diluent may increase high-solid content in alkyd formulation. It is not only serves as a solvent, but participates in film forming by taking part in the curing process. Low viscosity and volatility, good compatibility with binder and able to polymerize either by homopolymerization or copolymerization with alkyd are those properties of good reactive diluent. The reactive diluent that has been derived from renewable resources for example seed oils may provide biodegradable properties to the coating film thus increase the environmental benefits (Tiwari et al., 2016). Moreover, another advantages of reactive diluent over common solvent is the high buildup in a single application, minimization of surface defects owing to the absence of solvents, excellent heat and chemical resistance, and cost-effective for overall applications (Elvers, 2016). The uses of UV-curing process instead of traditional thermal curing can intensely reduce the greenhouse gas emissions by up to 90% because the energy supplies for thermal curing were found to be five to nine times higher than UV curing in the same processes (Dong et al., 2018).

Besides, the speed of cure is one of the exclusive advantages of UV-curable coatings over thermally curable coatings. Typically, a UV-curable coating can be cured within seconds, thus more economical compared to the conventional coatings that need hours or even days to dry completely. The quasi-instant hardening of clear or pigmented coatings, adhesives, and composites can be achieved in this UV curing system (Bruen, 2004; Decker, 1992).

Figure 2.5 compares the curing mechanisms between physical drying of thermally cured coatings and chemical curing when coatings are UV-irradiated. The UV curing system involves chemical curing with crosslinking reaction. In physical drying,

there are solvent evaporations and no crosslinking occurs after coatings are heated. On the contrary, chemical curing often involves minimal, if any, solvent evaporation. During UV irradiation, chemical polymerization and crosslinking take place to produce an extensive network of cross-linked polymer chains that lead to improved mechanical and chemical resistance of the coating films (Bruen, 2004; Schwalm, 2007).

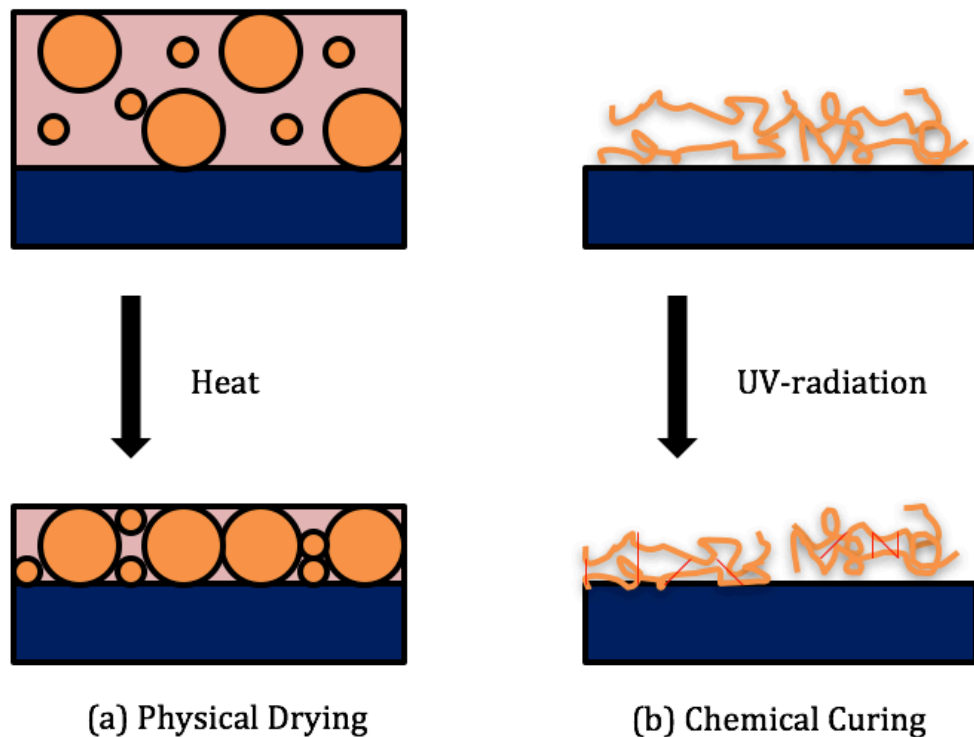


Figure 2.5: Curing mechanisms of (a) physically drying coating and (b) chemically curing coating

(Adopted from: Bruen, K., Davidson, K., Sydes, D. F., & Siemens, P. M. (2004). Benefits of UV-curable coatings. European coatings journal, 4, 42-56)

2.4.4 Applications

The most conventional method to cure coatings were air and oven drying (Islam et al., 2014; Saravari et al., 2005). However, this physical and thermal curing process involved harmful solvent that could lead to inconveniences such as thermal shrinkage and the release of environmental pollutant. Therefore, UV-curing technology was introduced because it has many benefits in coatings industry. One of the unique advantage from this system is the speedy hardening and involved solvent-free resin only. This process can be done at ambient temperature and resulting a high crosslinked polymer while presenting a good resistance to chemicals and heating. Besides, this technology showing dimensional stability after curing compared to thermal curing (Park et al., 2004). The UV-curable epoxy acrylate/methacrylates synthesized by Chattopadhyay and friends require only 8 s under UV radiation for being fully cured (Chattopadhyay et al., 2005). In separate work, a UV-curable clay-based nanocomposite polymer have been synthesized by photoinitiated crosslinking polymerization of acrylate and epoxy functionalized oligomers. This solvent-free resin containing a small amount (3 wt%) of organophilic clay was cured within 2 to 6 s only and the final conversion was found to be notably higher from 85 to 98 % based on coatings thickness (Decker et al., 2005).

In them of thermal stability, researchers have found that the UV-cured polymer is relatively more stable than the thermally cured material. For example, Pitchaimari and Vijayakumar studies on thermal degradation kinetics by comparing thermal and UV-cured N-(4-hydroxy phenyl) maleimide derivatives. During UV-curing process, the maleimide can absorb UV light and give an excited complex. The generation of the initiating radicals which were the excited maleimide from a donor molecule such as an acrylate/methacrylate monomer would react with one another and form a high crosslinked structure in the presence of UV irradiation. Hence, the high crosslinked

polymers were formed in these UV-cured polymers but not in thermally cured polymers. Besides that, they also found that maleimide/vinyl ether systems can be cured swiftly upon exposure to UV or electron beam source, to form crosslink network (Pitchaimari & Vijayakumar, 2014).

The UV-cured and non-cured films also can be compared based on the topography and roughness value of the film surfaces by employing atomic force microscopy (AFM). Based on the recent Yun and companions work, the AFM analysis results denoted that the surface roughness of crosslinked film was lower after UV curing process and pores that can absorb H₂O molecules were formed. Moreover, the films that have been UV cured for 20 min possess optimal physical and thermal properties compared to that of non-cured films (Yun et al., 2017).

There is a study regarding the curing speed of two UV-curable tung oil-based resins which were UV-curable tung oil (UVTO) and UV-curable tung oil based alkyd (UVTA) that were synthesized via a Diels–Alder cycloaddition. Here, the UV-curable tung oil alkyd was formulated with a free radical reactive diluent, tripropylene glycol diacrylate (TPGDA) and photoinitiator Irgacure 2100. Both resins were photocurable but the formula of UVTA exhibiting a faster curing speed than the formula of UVTO based on the DSC thermogram as shown in Figure 2.6. At initial exposure time, the exotherm implied that the polymerization of UVTO and UVTA have occurred, and then steadily decreased due to termination reaction. This finding will support the advantages of alkyd over pristine oil in UV-curing system (Thanamongkolit et al., 2012).

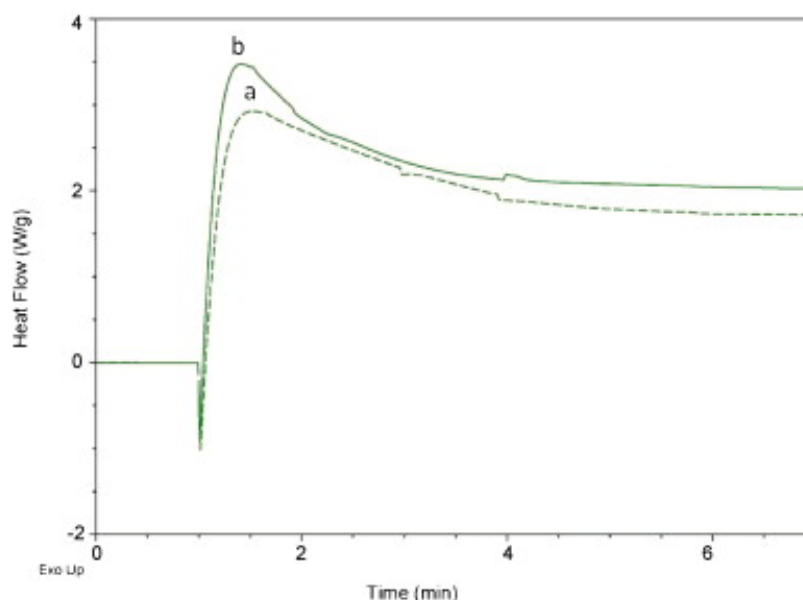


Figure 2.6: Thermograms of (a) UV-curable tung oil (UVTO) formula and (b) UV-curable tung-based alkyd (UVTA) formula

2.5 Corrosion and anti-corrosive coating

The deterioration of materials by chemical or electrochemical reactions with environment are known as corrosion. Corrosion occur in the presence of metallic conductor and electrolyte solution with different potential of anode and cathode region. In corrosion process, the corroded iron and steel will form rust product known as ferrous oxides. Besides, other examples of corrosion products are white rust and green-colored patina produced by zinc and copper respectively. There are three factors contributed to many forms of corrosion. First is the nature of corrodent that classified corrosion as wet or dry. Wet corrosion involves liquid or moisture while dry corrosion commonly required high-temperature gases in the reaction. The second factor to classify corrosion in different form is the mechanism of corrosions whether electrochemical or direct chemical reactions while the third factor are based on the appearance of the corroded metal either uniform or localized (Davis, 2000).

Corrosion is dangerous and may lead to several bad effects such as collapse of building and bridges, break of pipelines and leak of chemical plants. Other harmful

effects may arise from corroded electrical contacts that cause fire and blood poisoning due to the corroded medical implants. Additionally, these metallic corrosion results in huge economic losses per year worldwide. Figure 2.7 shows a case study in Beijing regarding on the economic loss from corrosion of materials over 10 years. From 2000 until 2002, the trend of the economic loss is almost constant around 10×10^8 CNY (China Yuan). However, the trend gradually increase starting from 2003 up to 2011 with huge economic loss about 22×10^8 CNY (Chen et al., 2013). Three types of materials are observed in term of corrosion and the most affected material is galvanized steel followed by painted steel and marble. In order to overcome negative impacts from corrosion, there are many innovation in anticorrosive coatings being developed recently including the introduction of nanoparticles and inhibitive materials in coating films. These several types of anticorrosive coatings can be differentiated by the composition of the coatings and their protective mechanisms.

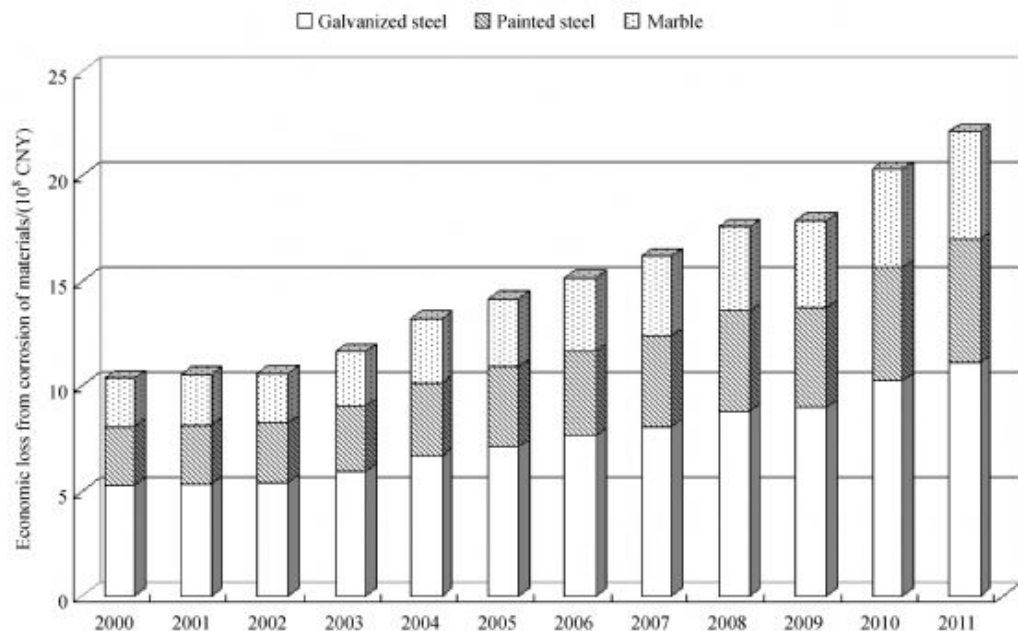


Figure 2.7: Economic loss from corrosion of materials in Beijing

(Source: Chen, C., Su, M., Liu, G., & Yang, Z. (2013). Evaluation of economic loss from energy-related environmental pollution: a case study of Beijing. *Frontiers of Earth Science*, 7(3), 320-330)

2.5.1 Components in anticorrosive coating

The anticorrosive-coatings are usually made up of multiple layers, such as primer, intermediate coat and topcoat. Coating compositions can vary greatly depending on the required properties and purposes of the coating. For example, in highly corrosive marine environments, the primer used for the coating should protect the substrate from corrosion and have good adhesion to the substrate. Therefore, metallic zinc or inhibitive pigments are usually included into the primer for coating structure that has exposed to the splash zone or atmospheric environment. For intermediate coat, a good adhesion between the primer and the topcoat should be the most important properties. Here, the thickness of the coating system may be increases while the transport of destructive species into the surface of the substrate could be inhibited. Topcoat, the most exposed part of coating to the environment may carry color and gloss. This layer should have high resistance towards environmental degradation that could shorten the lifetime of the coating through moisture and temperature.

2.5.2 Protective mechanism

There are three types of protective mechanism of anti-corrosive coatings against corrosion simplified in Figure 2.9; barrier effect, inhibitive effect (passivation of substrate surface) and galvanic effect (sacrificial protection) (Sørensen et al., 2009). Barrier protection uses a coating system with low permeability of liquids, ions and gases in order to block the carriage of aggressive species into the surface of the substrate. This ionic impermeability of barrier coatings ensures a very high electrical resistance of moisture at the interface of the coating-substrate. By that, the transfer of corrosion current between the anode and cathode is reduced since there are low conductivity of the electrolyte solution at the substrate. The coating thickness and the nature of the binder are those dependent properties that influence the degree of protection in this barrier coating system. Coating with high thickness may behave as semipermeable

membranes thus reduced the delamination of defect-free and artificially damages on the barrier coatings. Inert pigmentation such like titanium dioxide, micaceous iron oxide and glass flakes are examples of typical barrier coatings. They usually applied in lower volume concentration and may be used as primer, intermediate or topcoat.

For inhibitive effect, a chemical conversion layer or the addition of inhibitive pigments to the coating would make the passivation of the substrate surface being achieved. In order to achieve the effectiveness in this system, the inhibitive coatings are applied as primers so that the dissolved constituents can react with the metal. Therefore, this type of protective coatings are usually applied to substrates with a risk of atmospheric corrosion but not for immersion in water or burial in soil. One of the polymer that has been extensively studied as anti-corrosive coating through passivation is polyaniline. Based on Figure 2.8, the passivation of PANI occur when there is interaction between PANI and substrate forming a protective oxide layer on the metal. In neutral media, the oxygen is reduced on the coating while the ferrous iron is oxidized to iron oxides at the pin hole area, which is the exposed iron surface under the coating. The reduction of oxygen into hydroxide may stabilize the polymer from cathodic disbonding by shifting the metallic surface to polymer-electrolyte interface. On the other hand, the passivation of pin hole in acid media are happen by conversion of conducting emeraldine salt to non-conducting leuco-emeraldine salt of PANI (Deshpande & Sazou, 2016).

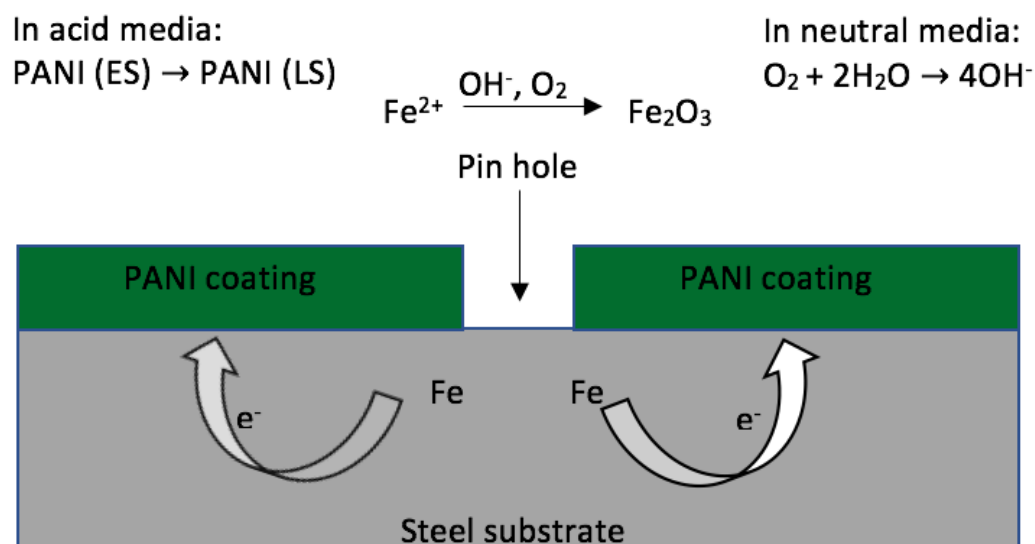


Figure 2.8: Schematic diagram of mechanism of passivation by PANI on steel

(Adopted from: Sathiyarayanan, S., Muthukrishnan, S., Venkatachari, G., & Trivedi, D. C. (2005). Corrosion protection of steel by polyaniline (PANI) pigmented paint coating. *Progress in Organic Coatings*, 53(4), 297-301)

Galvanic effect as protective mechanism for anticorrosive coatings can be obtained by sacrificial corrosion of more electrochemically active metal either organic or inorganic that was in electrical contact with the substrate. This type of protective coatings also applied as primers same as inhibitive coatings since direct contact with substrate is necessary so that electrical contact between the substrate and the sacrificial metal is obtained. Coatings with metallic zinc powder as additives is the most widely studied since they provide excellent corrosion protection on the steel. Anodic active coating is produced with the presence of zinc. Metal as cathode is protected by the sacrificial zinc as the anode. Here, the transfer of galvanic current by zinc primer plays important role to resist towards corrosion with consistent conductivity in the system and sufficient zinc amount.

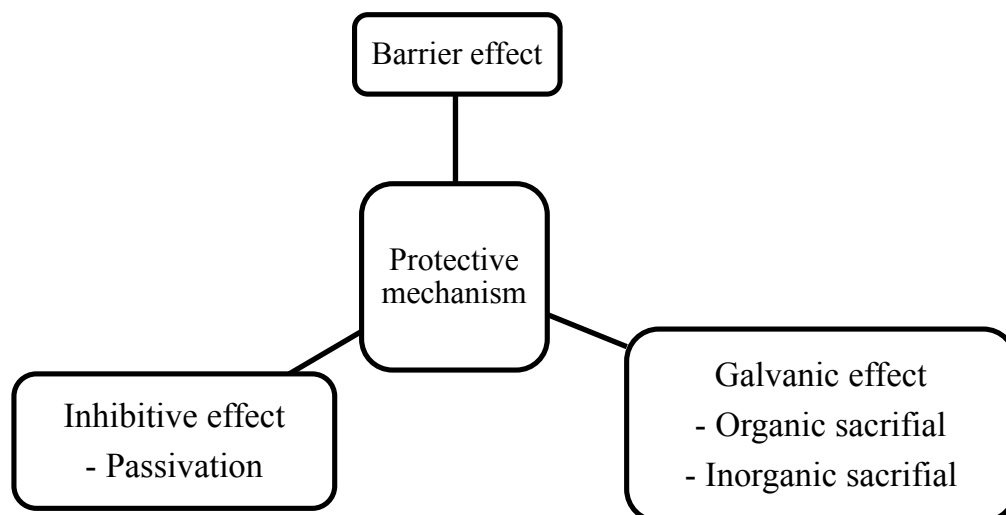


Figure 2.9: Protective mechanisms of anticorrosive coatings

2.6 Conductive coating

Commonly, there are certain amount of metal content prepared in conventional conductive coatings. Recently, silver (Ag) coatings broadly use in medical materials for example wound bandages, mainly due the ability of Ag ion to release in aqueous media for targeted antibacterial properties. Moreover, Ag-coated fibers also have been used for sensing applications such as electrocardiography (ECG) belts since they could offer excellent electrical properties (Amberg et al., 2018). However, this beneficial Ag metal was not cost-effective. In other applications, the more economical metals such as copper and nickel used to replace the pricey metals but still facing problems on oxidation, sedimentation, while being hazardous and harmful to the environment and end-users (Wissling, 2006). As an alternative in electrically conductive coatings, these metals were replaced by conducting polymers. Most of the conducting polymers were reported to have high chemical and thermal stability thus suitable to be incorporated into coating (Alam et al., 2009). Conductive polymer nanocomposites have many potential applications and extensively play roles in sensors, solar cells, energy storages, and

energy savings applications (Giuri et al., 2016; Jin et al., 2016; Liu et al., 2017; Liu et al., 2016; Yang et al., 2015).

Alhashmi newly work on a simple method to fabricate highly electrically conductive cotton fabric using poly(3,4-ethylenedioxythiophene):poly(styrenesulfonate) (PEDOT:PSS) without any metals or nanoparticles. Conventional method usually involved metal such as indium tin oxide, ITO and copper. However, this method used DMSO doping, a commercial PEDOT:PSS solution and cotton fabric only. He reported that the treatment of cotton fabric with different PEDOT:PSS concentrations showed significant improvement in conductivity. A minimum sheet resistance value of $1.58 \Omega/\text{sq}$ was obtained with the concentrated PEDOT:PSS treatment in the conductive cotton fabric. This process was concluded as an easy, energy-saving and environmentally friendly technique to produce electrically conductive cotton with a conducting polymer (Alamer, 2017).

Besides, other conducting polymer such as polyaniline (PANI) usually integrated into coatings to show its potential applications in electromagnetic interference (EMI) shielding and giant magnetoresistance (GMR) sensors (Guo et al., 2016; Preeti et al., 2017; Pritom et al., 2017; Zhu et al., 2012). PANI also has excellent electrical conductivity and is usually reported as anti-corrosive coating films in many studies (Bhadra et al., 2009; Kalendová et al., 2008; Twite & Bierwagen, 1998). Besides, other conductive polymer nanocomposite for example polyurethane multiwalled carbon nanotube, Co-doped TiO_2 /polypyrrole, and micro/nanocapsules for self-healing coatings also reported to have anti-corrosion properties (Ladan et al., 2017; Wei et al., 2013; Wei et al., 2015). Furthermore, there are some works reported the ability of conducting polymer to improve corrosion resistance of conventional thermal curable coatings (Alam et al., 2009; Martí et al., 2012).

CHAPTER 3: METHODOLOGY

3.1 Materials

Refined, bleached and deodorized (RBD) palm olein obtained from Yee Lee Edible Oils Sdn. Bhd. (Perak, Malaysia) was used without further treatment. Glycerol (99.5%), maleic acid (MA) and methyl methacrylate (MMA) were purchased from Friendemann Schmidt (Parkwood, Western Australia) while phthalic anhydride (PA) from R&M Chemicals (United Kingdom). Sodium chloride (NaCl), $\text{Ca}(\text{OH})_2$ and hydrochloric acid (HCl) 37% were purchased from System, HmbG Chemicals and RCI Labscan Limited (Bangkok, Thailand) respectively. Polyaniline (emeraldine salt), trimethylolpropane triacrylate (TMPTA) and benzophenone (99%) were procured from Sigma-Aldrich (Steinheim, Germany). M-cresol and sodium hydroxide (NaOH) were gained from Merck (Darmstadt, Germany) and Macron (Sweden) respectively.

3.2 Characterizations of palm olein

3.2.1 Fourier transform infrared spectroscopy (FTIR)

Palm olein was spread into thin film on KBr cell. IR spectrum of palm olein was recorded using Perkin Elmer spectrometer from wavenumber 400 to 4000 cm^{-1} at a resolution of 4 cm^{-1} .

3.2.2 Proton nuclear magnetic resonance spectroscopy (^1H -NMR)

^1H -NMR spectrum of palm olein was recorded using FT-NMR Avance III 400 MHz spectrometer. The palm olein was dissolved in deuterated chloroform prior to the analysis, and the signal was locked at 0 ppm with tetramethylsilane (TMS).

3.3 Synthesis of alkyd

Alkyd synthesis consists of two stages and this method was adopted from Ang and Gan's work (Ang & Gan, 2012). First stage was begun with transesterification of 306.6 g of palm olein and 167.9 g of glycerol, using 0.25 g (0.08 wt%) of Ca(OH)_2 as catalyst. The palm olein was expected to be converted to a predominant mixture of monoglyceride in this step. The reaction mixture was constantly stirred at 200 rpm throughout the cooking process in order to have a homogenous mixing of reactants. Temperature of reaction mixture was controlled and monitored using a heating mantle and digital thermometer. The reaction mixture was heated at 230°C for 2 h before cooling down to 150°C . Then, diacids; 179.0 g of phthalic anhydride and 51.0 g of maleic acid were added into the reaction mixture and the polycondensation process was carried out at 220°C until the acid number dropped below 10% of the initial value.

Figure 3.1 shows the experimental set up for alkyd cooking. The set up for the first stage of transesterification process was shown in Figure 3.1 (a), a Liebig condenser was attached to the reaction flask to avoid volatile reactants or products escape to the environment and to control pressure flow in the flask. The set up for the second stage which was the polycondensation process was shown in Figure 3.1 (b), a modification with Dean-Stark trap was attached between the reaction flask and condenser to collect the water produced thus forward equilibrium of formation of alkyd was favored (Wutticharoenwong et al., 2012).

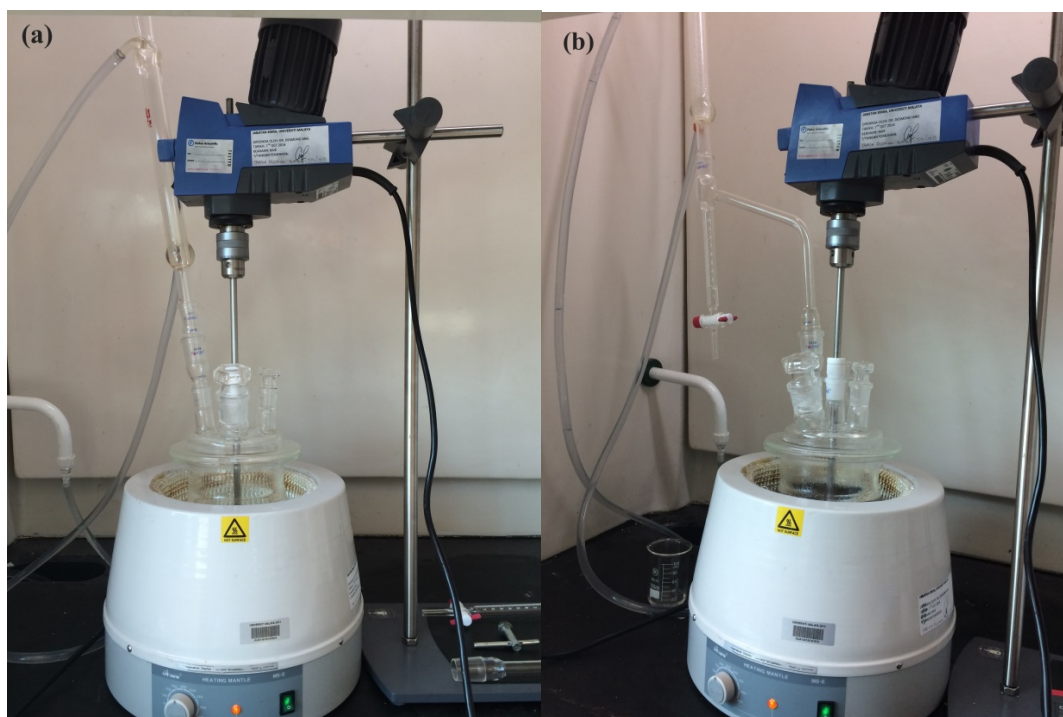


Figure 3.1: Experimental set-up for (a) First stage of alkyd cooking; transesterification, and (b) Second stage of alkyd cooking; polycondensation.

3.4 Characterizations of alkyd

3.4.1 Determination of acid number

The acid number of alkyd was obtained based on standard test method for acid value of organic coating materials, ASTM D1639 - 90. Neutral solvent comprised of equal volume of isopropanol and toluene was used to dissolve the alkyd. Then the solution was titrated with standardized KOH solution using phenolphthalein as the indicator. The acid value test was done in duplicate and the acid number was calculated using the following formula:

$$A = \frac{VK}{S \times N} \quad (\text{Eqn. 3.1})$$

Where; A = acid value

V = volume of KOH solution required for titration of sample, mL

K= weight of KOH per mL of KOH solution, mg

S = sample weight, g and

N = non volatile content of sample

3.4.2 FTIR spectroscopy

Alkyd was applied into a thin film on KBr cell. IR spectrum of alkyd was recorded using Perkin Elmer spectrometer from wavenumber 400 to 4000 cm^{-1} at a resolution of 4 cm^{-1} .

3.4.3 ^1H -NMR spectroscopy

Alkyd was dissolved in deuterated chloroform prior to the analysis, and the signal was locked at 0 ppm with tetramethylsilane (TMS). ^1H -NMR spectrum of the alkyd was recorded using FT-NMR Lambda 400 MHz spectrometer.

3.4.4 Thermal analysis

Thermal properties of the alkyd were studied using thermal gravimetric analyzer (TGA 6, Perkin Elmer), where the sample was heated from 50°C to 900 °C at 20 °C/min in N_2 atmosphere.

3.5 Characterizations of polyaniline (PANI)

3.5.1 FTIR spectroscopy

PANI powder was characterized using ATR-FTIR machine. The scan was done from wavenumber 400 to 4000 cm^{-1} at a resolution of 4 cm^{-1} .

3.5.2 Ultraviolet-visible spectroscopy

UV-Vis analysis was referred to Singh and Choudhary method (Singh & Choudhary, 2016). PANI powder was dissolved in m-cresol and then UV-cured as the thin film on the glass. The film was scanned with UV-Vis (UV-2600) spectrophotometer in the range of 300 to 900 nm.

3.5.3 Conductivity test

The conductivity test was performed on compressed PANI powder in the range of 10^{-7} to 10^7 S/cm using four point probe, Loresta HP. The PANI powder was compressed using a constant load of 100 kg and took around 10 min to form pellet with a diameter of 10 mm and thickness of 0.8 -1.1 mm.

3.5.4 Thermal analysis

Thermal properties of the PANI were studied using thermal gravimetric analyzer (TGA 6, Perkin Elmer), where the sample powder was heated in N₂ atmosphere from 50°C to 900 °C at 20 °C/min.

3.6 Preparation of alkyd/PANI coating

3.6.1 Preparation of coating mixture

Coating mixture A was prepared with 45% of alkyd, 45% of MMA as reactive diluents and 10% of TMPTA, followed by addition of six parts per hundred (phr) benzophenone as UV photoinitiator. The mixture was stirred until homogenized. Other separate sets of coating mixtures which were B, C, D, E, and F were prepared using the same procedure as above but with the addition of different amounts of PANI and 0.5 g m-cresol as shown in Table 3.1. The ratio 5:5 is not used in this formulation because coating with this ratio has exceed limitation of PANI content which is the coating starts to become brittle and has poor adhesion. Separate coating mixtures L and M were prepared with lesser amounts of PANI (0.5 and 1% PANI respectively) for the purpose of studying the corrosion resistance through EIS.

Table 3.1: Compositions of coating mixtures

Coating Mixture	Amount / g					Ratio	PANI loading in coating mixture (wt%)
	Alkyd	MMA	TMPTA	PANI	M-cresol	Alkyd: PANI	
A	7.50	7.50	1.67	0.00	0.00	10 : 0	0.0
B	7.50	7.50	1.67	0.83	0.50	9 : 1	4.6
C	7.50	7.50	1.67	1.32	0.50	8.5 : 1.5	7.0
D	7.50	7.50	1.67	1.88	0.50	8 : 2	9.9
E	7.50	7.50	1.67	3.21	0.50	7 : 3	15.8
F	7.50	7.50	1.67	5.00	0.50	6 : 4	22.6

3.6.2 Treatment of mild steel

Toluene was used to remove any oil or stains on mild steel panels. Steels were treated first by pickled in concentrated acid, H_2SO_4 followed by rinsed with distilled water and dried. Then, steels were polished with several grades of emery papers from P600, P800, P1200, P1500 until P2000. Next, they were degreased with acetone, rinsed with distilled water and dried.

3.6.3 Application and curing of coatings

Coating mixtures were applied on mild steel panels using baker film applicator from TQC and cured under UV light from Electro-Lite Corporation (Electro-Cure 4001) using a 400W lamp that radiates UV light ($\lambda=365nm$) at intensity of $125mW/cm^2$ as shown in Figure 3.2. The films were irradiated until they were no longer tacky to touch.

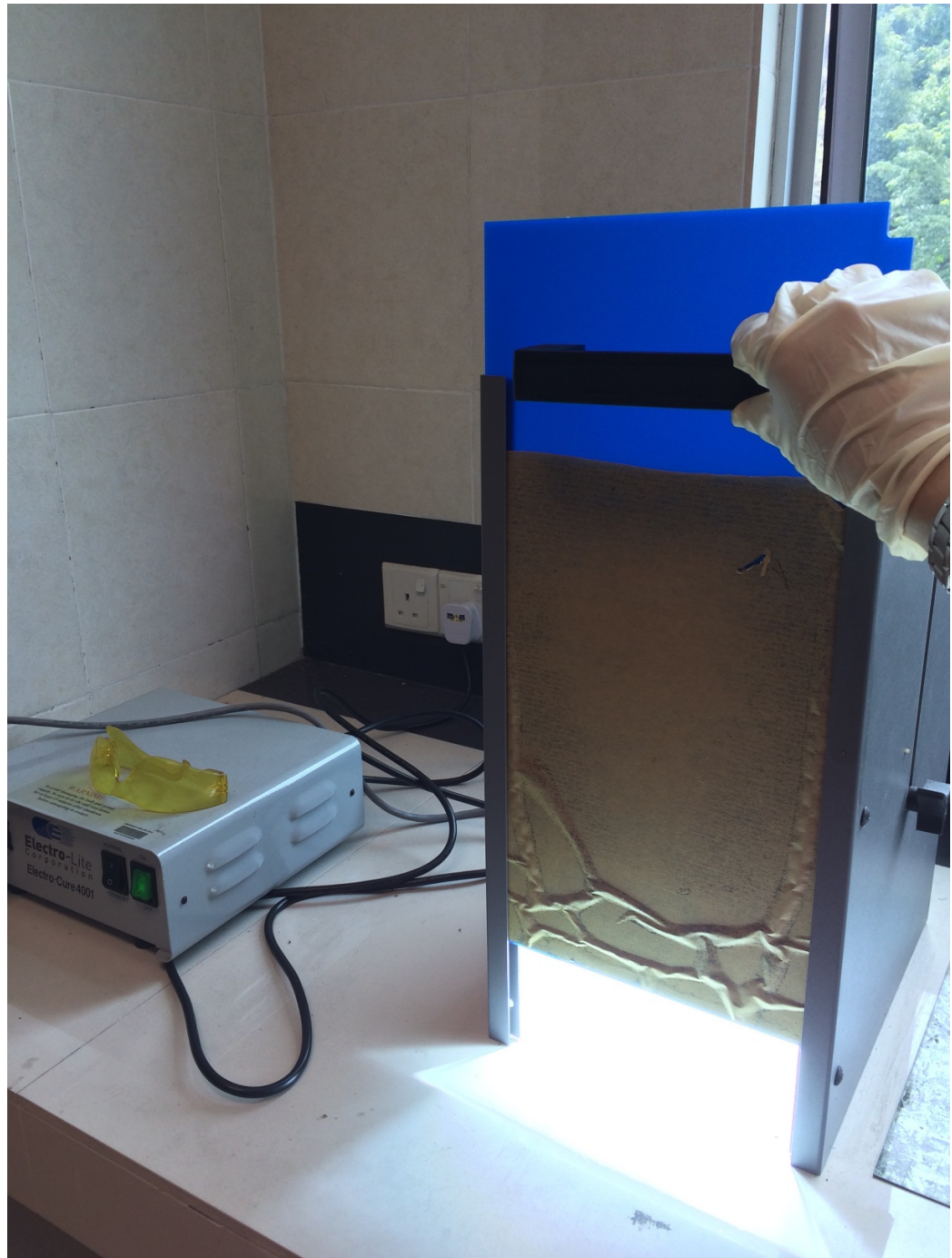


Figure 3.2: UV curing machine

3.7 Film properties of cured coatings

3.7.1 Pencil hardness test (PHT): ASTM D3363 - 00

Pencil hardness test was conducted to determine the film hardness of the coatings. A coated mild steel with alkyd/PANI coating was placed on a horizontal surface. A pencil from a set of 20 Koh-i-noor pencils was clamped in the TQC pencil hardness test instrument at an angle of 45° from the coating surface as shown in Figure 3.3. Then, the instrument was pushed away from the operator in a stroke. The process was started with the hardest pencil, grade 6H and continued down the scale of hardness then stopped when the pencil not scratched the film. The pencil hardness scale was shown in Figure 3.4. This step was repeated at three different area of panel and the hardest pencil grade that fails to scratch the coating was recorded.



Figure 3.3: TQC pencil hardness test instrument

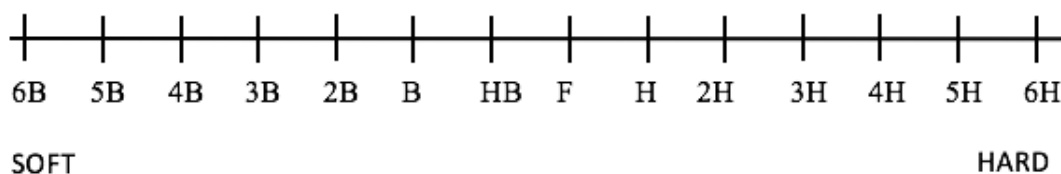
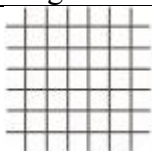
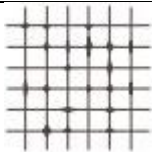
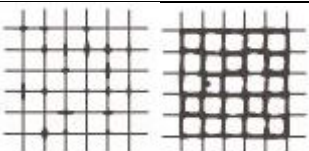
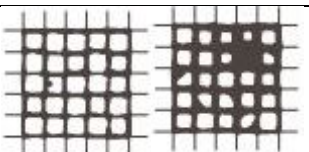
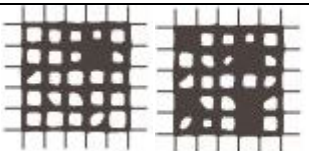
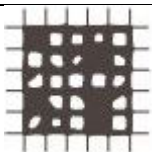


Figure 3.4: Pencil hardness scale

3.7.2 Crosshatch adhesion tape test: ASTM D3359 - 97

As for the film adhesion, the test was conducted using cross-hatch tape test using 3M Scotch 530 tape. A hatch consisting of 11 intersecting vertical and horizontal lines with 1 mm apart was carved on the cured coating using a blade. Any detached flakes or ribbons of the coating at the hatch were gently brush off using a brush. A tape was placed on the hatch and then peeled off in a stroke at an angle approximately 180° . The results were reported in terms of % film removal and classified into 6 different classes as shown in Table 3.2.

Table 3.2: Classification of adhesion test results

Classification	Film removal (%)	Surface of cross-cut area from which flaking has occurred
5B	0	
4B	< 5	
3B	5 - 15	
2B	15 - 35	
1B	35 - 65	
0B	> 65	

3.7.3 Water and alkali resistance test: ASTM D1647 - 89

For water and alkali resistance test, the coating mixtures were applied on glass panels using spin coating technique with a spin coater (Model: Spin 150, Germany) and cured under UV light. The water resistance test was conducted by partially immersing the coated glass panels in distilled water for 24h. The coating samples were then removed and dried at room temperature. Any presence of whitening on the films, and the time taken for the whitening to disappear were recorded.

In alkali resistance test, all coatings on glass panels were half immersed in aqueous NaOH solution (30g/L) and the time needed for film defects to be apparent was recorded.

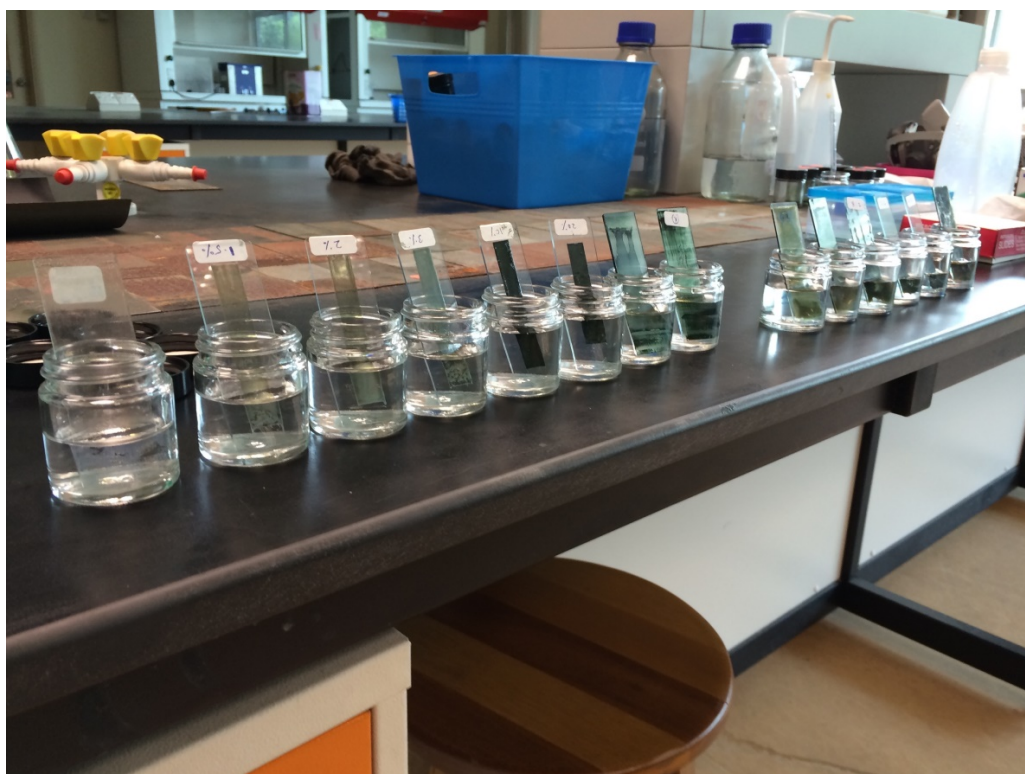


Figure 3.5: Water and alkali resistance test set-up

3.7.4 Acid resistance and salt water resistance tests

Another chemical resistance tests; acid and saltwater resistance tests were conducted based on (Ang, 2015). The coated glass panels were immersed in 0.1M HCl solution and 5% w/w NaCl solution respectively for 1h. Both solutions were preheated until 80°C in water bath in order to have constant temperature throughout the tests. All the panels were removed and rinsed with distilled water after 1h and observe for any film defects.

3.7.5 Ultraviolet-visible spectroscopy

UV-Vis analysis of alkyd & alkyd/PANI coatings were conducted by coat each of the coating mixtures on the glass slide. Then the coatings were UV-cured as the thin film on the glass and scanned with UV-Vis (UV-2600) spectrophotometer in the range of 300 to 900 nm.

3.7.6 Thermal Analysis

Thermal degradations of the coatings were studied using thermal gravimetric analyzer (TGA 6, Perkin Elmer). The UV-cured coatings A, D, E and F on mild steels were scrapped off and then scanned from 50 to 900 °C at 10 °C/min, 20 °C/min and 30 °C/min in N₂ atmosphere. The activation energy of decomposition, E_d of the coating films were determined using the derivative of TGA thermograms of coatings.

3.8 Development of UV-curable alkyd/PANI coating

3.8.1 Effect of coating composition (Alkyd:PANI) on film conductivity

Alkyd coatings containing different proportion of PANI as shown in Table 3.1 were coated on glass slides. All coating films were cured under UV light for 120s. Conductivity test was performed on the UV-cured coatings in the range of 10⁻⁷ to 10⁷ S/cm using four point probe, Loresta HP.

3.8.2 Effect of UV curing time on film conductivity and FTIR analyses

In order to study the effect of UV curing time on film conductivity, coating F with the highest percentage of PANI was chosen and irradiated with UV light for 0, 30, 60, 90 and 120 s. Conductivity test was performed on the UV-cured coatings in the range of 10^{-7} to 10^7 S/cm using four point probe, Loresta HP. FTIR analyses on the films were conducted using ATR-FTIR machine to study the plausible structural changes of the PANI that affected the conductivity. This method was adopted from Kawata and colleagues' study (Kawata et al., 2013).

3.9 Surface study and electrochemical methods

Two coating mixtures with a lesser amount of PANI were prepared for the corrosion study, where coating mixture L comprised of 0.5% PANI, and mixture M comprised of 1.0 % of PANI. Coating K served as a control and carried no PANI. The coating mixtures were coated on mild steels using dipped coating technique in order to have a very thin film for the electrochemical impedance spectroscopy (EIS) and linear polarization studies. Before the coatings is tested electrochemically, a surface study of field-emission scanning electron microscopy analysis (FESEM) is done on Coating K and Coating L. This study is done in order to compare the differences in term of morphology between surface coating of alkyd (Coating K) and surface coating of alkyd/PANI (Coating L). In electrochemical studies, coated mild steels were attached to EIS cell using alraldite for EIS measurement and filled up with 3.5% NaCl solution as the electrolyte as shown in Figure 3.6. The corrosion protection performances of coatings were investigated by variations of open circuit potential (OCP), EIS and Tafel analysis, performed on a potentiostat/galvanostat (Autolab PGSTAT30, Ecochemie Netherlands) as shown in Figure 3.7. The coated mild steel was used as a working electrode while graphite and saturated calomel electrode (SCE) were used as counter and reference electrodes, respectively. The OCP and EIS measurements were carried

out until 30 days of immersion in saline solution at room temperature. The frequency for EIS measurement was ranging from 100k Hz to 0.01 Hz. Recorded Nyquist and Bode plots of the impedance data were analyzed with the frequency response analyzer (FRA) software. The measurement of these electrochemical methods was adopted from the work of Ladan and companions (Ladan et al., 2017).

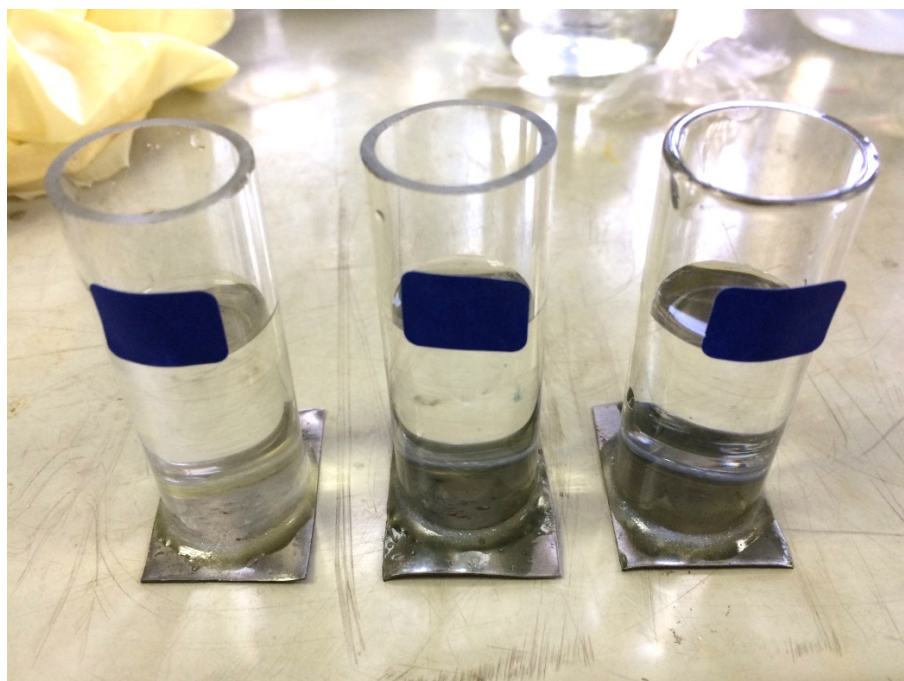


Figure 3.6: EIS cells of coated mild steels

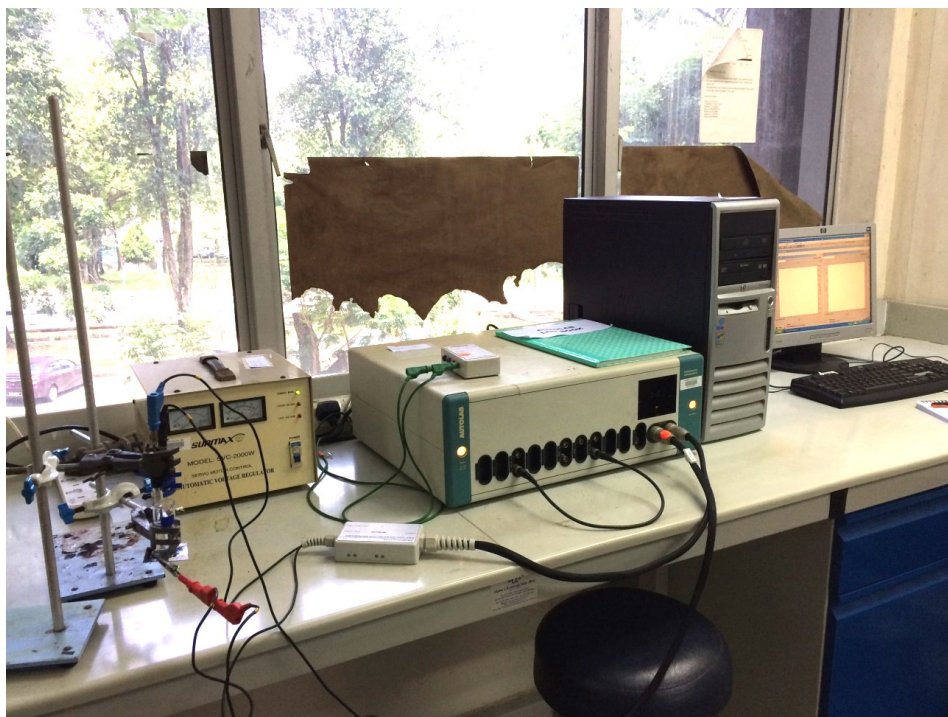


Figure 3.7: Set-up of electrochemical evaluation

CHAPTER 4: RESULTS AND DISCUSSIONS

4.1 Characterizations of palm olein

4.1.1 FTIR spectroscopy

Peaks present in FTIR spectrum of palm olein were assigned in Table 4.1 while the FTIR spectrum was shown in Figure 4.1. The spectrum shows intense peaks around 2924 and 2856 cm^{-1} which were characteristics of methyl ($-\text{CH}_3$), methylene ($-\text{CH}_2$) and methine ($-\text{CH}$) groups. Strong peak at 1744 cm^{-1} were due to $\text{C}=\text{O}$ of esters group and peaks around 1156 and 1100 cm^{-1} were due to $\text{C}-\text{O}$ stretching. The bands at 1452 and 1358 cm^{-1} may due to the angular deformation of asymmetric and symmetric methylene group ($-\text{CH}_2$) respectively. The band presents at 715 cm^{-1} may contributed by the vibration of aliphatic chains of fatty acids. Palm oil contains 40% oleic acid (monounsaturated fatty acid), 10% linoleic acid (polyunsaturated fatty acid), 45% palmitic acid and 5% stearic acid (saturated fatty acid). These percentages gives a balanced ratio of unsaturated and saturated fatty acids in palm oil (MPOC, 2012). However, the palm olein that fractionated from palm oil may contains higher levels of oleic acid (39–45%) and linoleic acids (10–13%) compared to the palm oil (Oil Palm Knowledge Base, 2014).

Table 4.1: Peak assignments for FTIR spectrum of palm olein

Wavenumber (cm^{-1})	Functional groups
2924, 2856	$-\text{CH}_3$, $-\text{CH}_2$ and $-\text{CH}$ stretch
1744	$-\text{C}=\text{O}$ ester stretch
1452, 1358	$-\text{CH}_2$ - bend
1156, 1100	$-\text{C}-\text{O}$ ester stretch
715	$-\text{CH}_2$ rocking (long chain band)

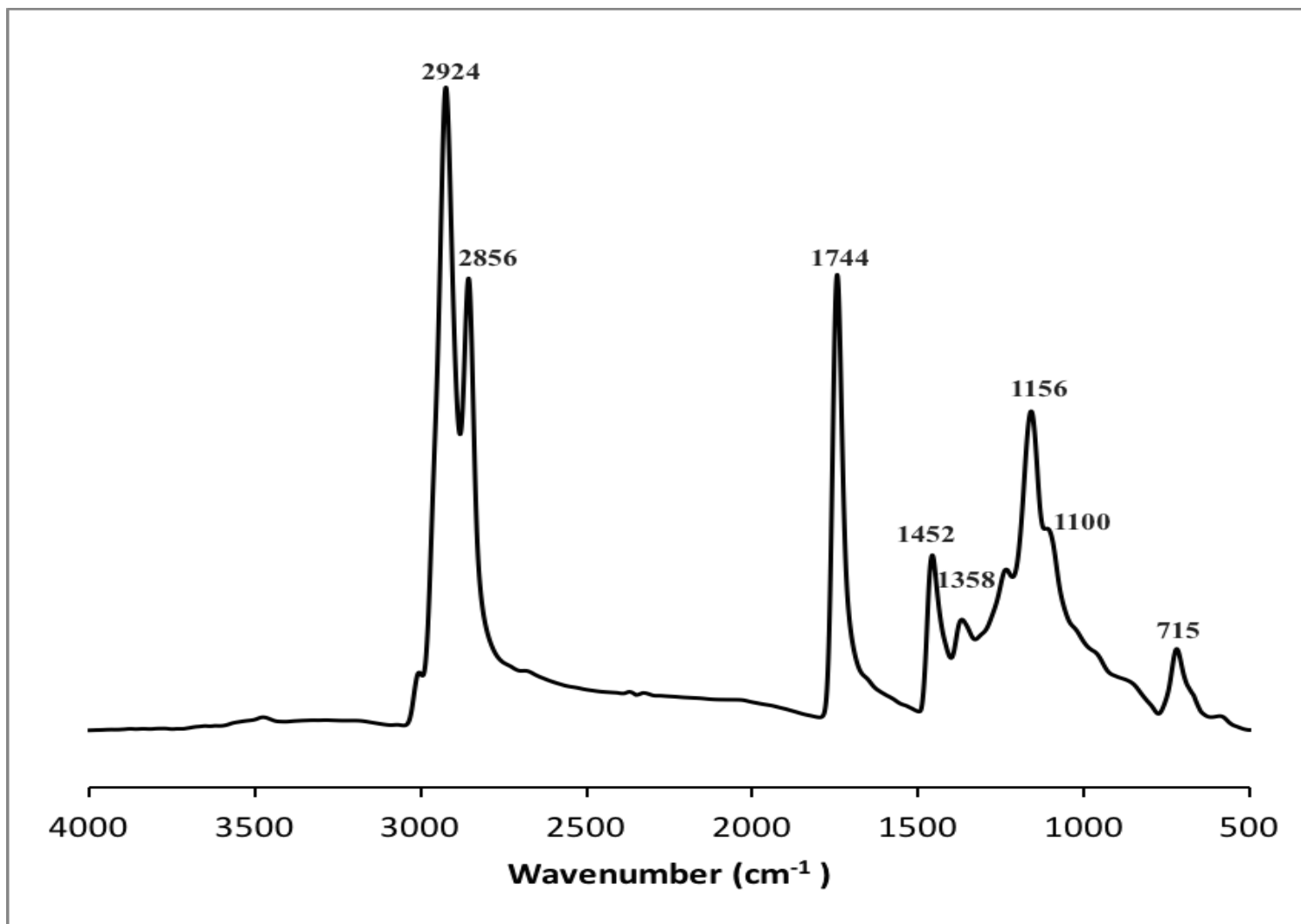


Figure 4.1: FTIR spectrum of palm olein

4.1.2 ¹H-NMR spectroscopy

Peaks present in ¹H-NMR spectrum of palm olein are assigned in Table 4.2 while the spectrum was shown in Figure 4.2. There are 3 characteristics peaks presenting the unsaturation in the oil. Peak at 5.3 ppm was observed as the result of the resonance of vinyl proton, $-HC=CH-$ that are present in unsaturated fatty acids such as oleic acid and linolenic acid. Allylic protons, $-C=C-CH_2-$ resonated at 2.0 ppm because of the deshielding effect from the C=C. At 2.7 ppm, a small peak was observed due to the resonance of protons in between two $-C=C-$ groups, $-C=C-CH_2-C=C-$. Other weak peaks are observed since major protons exist in linoleic acid that has low content in palm olein.

Table 4.2: Peak assignments for ¹H-NMR spectrum of palm olein

Chemical shifts / ppm	Types of protons
5.3	$-HC=CH-$
4.3 - 4.1	$-COO-CH_2-$
2.7	$-C=C-CH_2-C=C-$
2.3	$-OOC-CH_2-$
2.0	$-C=C-CH_2-$
1.6	$-OOC-CH_2-CH_2-$
1.3	$-R-CH_2-R-$
0.8	$-R-CH_3$

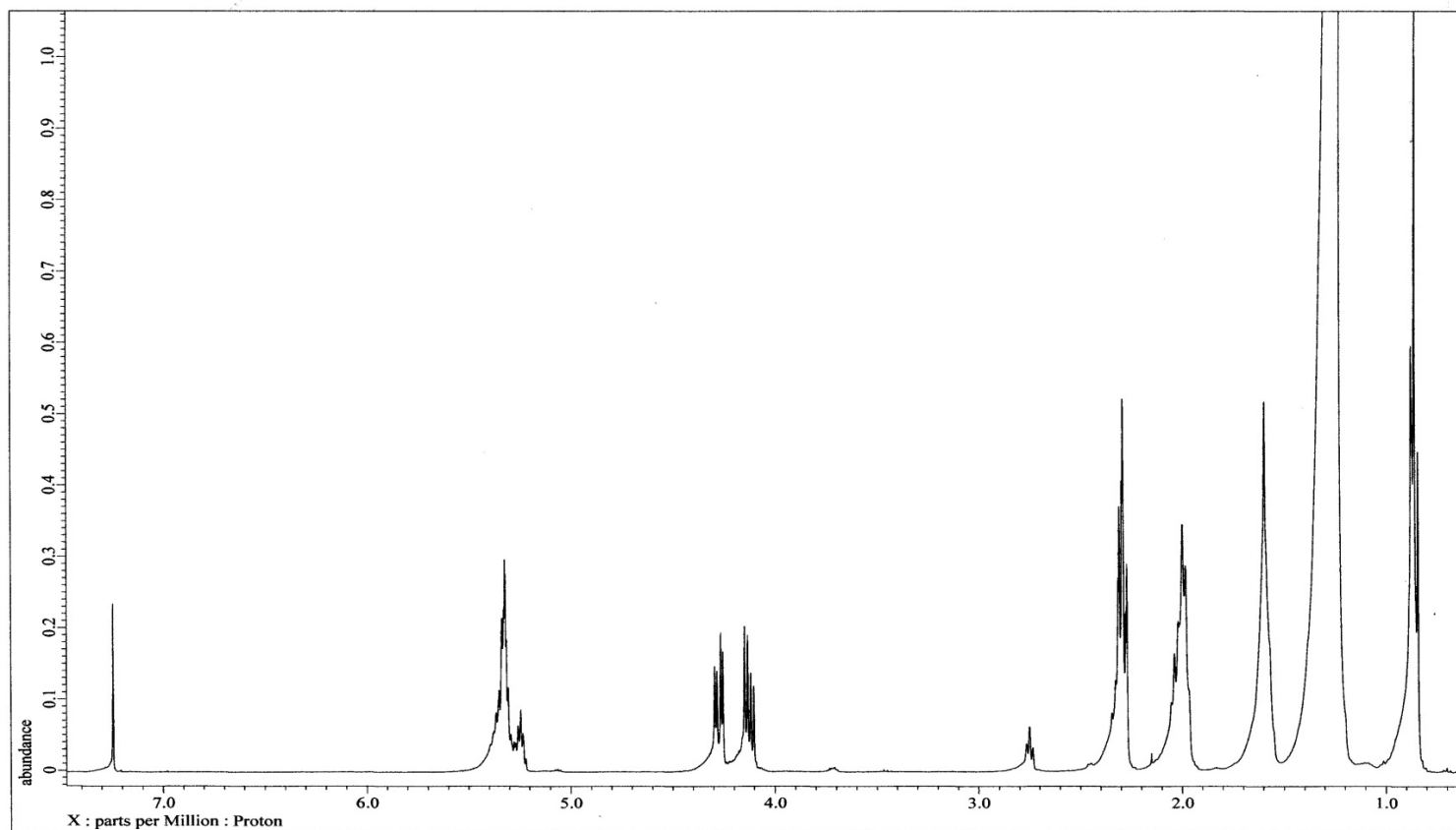


Figure 4.2: ^1H -NMR spectrum of palm olein

4.2 Characterizations of alkyd

4.2.1 Determination of acid number

The initial acid number of alkyd was obtained theoretically by calculation based on the amounts of acids introduced into the mixture which was 275 mg KOH/g alkyd. This acid number was decreased during alkyd cooking because of the conversion of –COOH to ester linkages. The acid number of reaction mixture was measured regularly started an hour after the diacids added in the reaction flask. Water was produced as a by-product of esterification process. The final acid number of alkyd was 24.9 mg KOH/g alkyd, which reflects greater than 90% conversion. The acid number of alkyd was calculated based on ASTM D1639 - 90 using the formula in Eqn. 3.1.

4.2.2 FTIR spectroscopy

FTIR spectrum of alkyd was shown in Figure 4.3, and the peaks present in the spectrum were summarized in Table 4.3. The broad band at 3464 cm^{-1} was due to OH-stretching. The intense peaks around 2925, 2854, 1734, 1284 and 1139 cm^{-1} have similar characteristics with palm olein spectrum as discussed before. Besides, a small peak at 1580 and 744 cm^{-1} are attributed to the aromatic rings while the presence of C=C- peak in the region 1647 cm^{-1} was attributed to the maleic acid moiety in the alkyd chain.

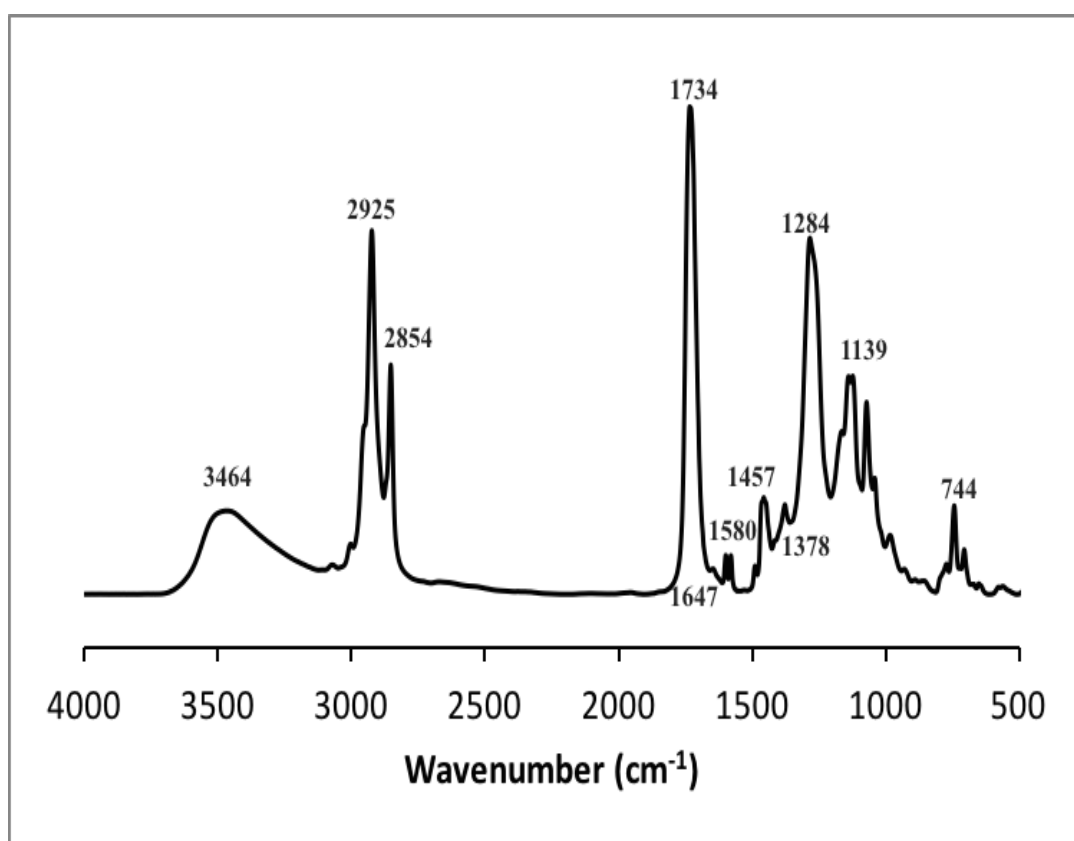


Figure 4.3: FTIR spectrum of alkyd

Table 4.3: Peak assignments for FTIR spectrum of alkyd

Wavenumber (cm ⁻¹)	Functional groups
3464	-O-H stretch
2925, 2854	-CH ₃ , -CH ₂ and -CH stretch
1734	-C=O ester stretch
1647	-C=C- stretch
1580	aromatic -C=C- stretch
1457, 1378	-CH ₂ - bend
1284, 1139	-C-O ester stretch
744	aromatic bend (ortho substituted)

4.2.3 ¹H-NMR spectroscopy

The result was supported by the ¹H-NMR spectrum of alkyd in Figure 4.4 showing peak at 6.92 ppm which corresponds to the resonance of -OOC-CH=CH-COO- protons of incorporated maleic acid. Similar results were reported by Ang and Gan in their work on maleated alkyd synthesis (Ang & Gan, 2012). Peaks in the ¹H-NMR spectrum were assigned and shown in Table 4.4. A plausible synthesis route of maleated alkyd was shown in Figure 4.5.

Table 4.4: Peak assignments for ¹H-NMR spectrum of alkyd

Chemical shifts / ppm	Types of protons
7.78, 7.58	Aromatic -CH=CH-
6.92	-OOC-CH=CH-COO-
5.41	-HC=CH-
4.41 – 3.68	-COO-CH ₂ -, -CH ₂ -OH
2.83	-C=C-CH ₂ -C=C-
2.40	-OOC-CH ₂ -
2.08	-C=C-CH ₂ -
1.67	-OOC-CH ₂ -CH ₂ -
1.34	-R-CH ₂ -R-
0.82	-R-CH ₃

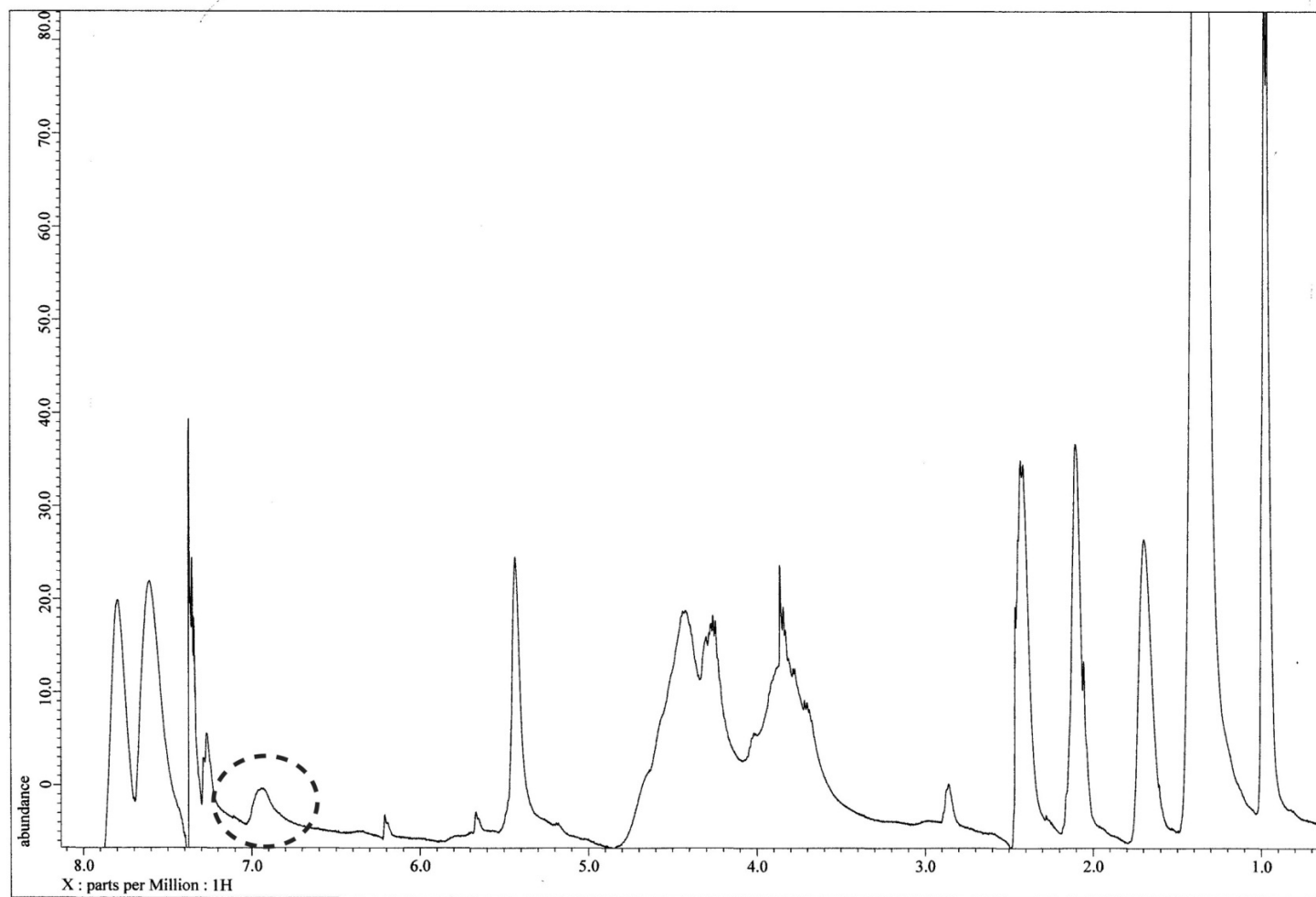


Figure 4.4: ^1H -NMR spectrum of alkyd

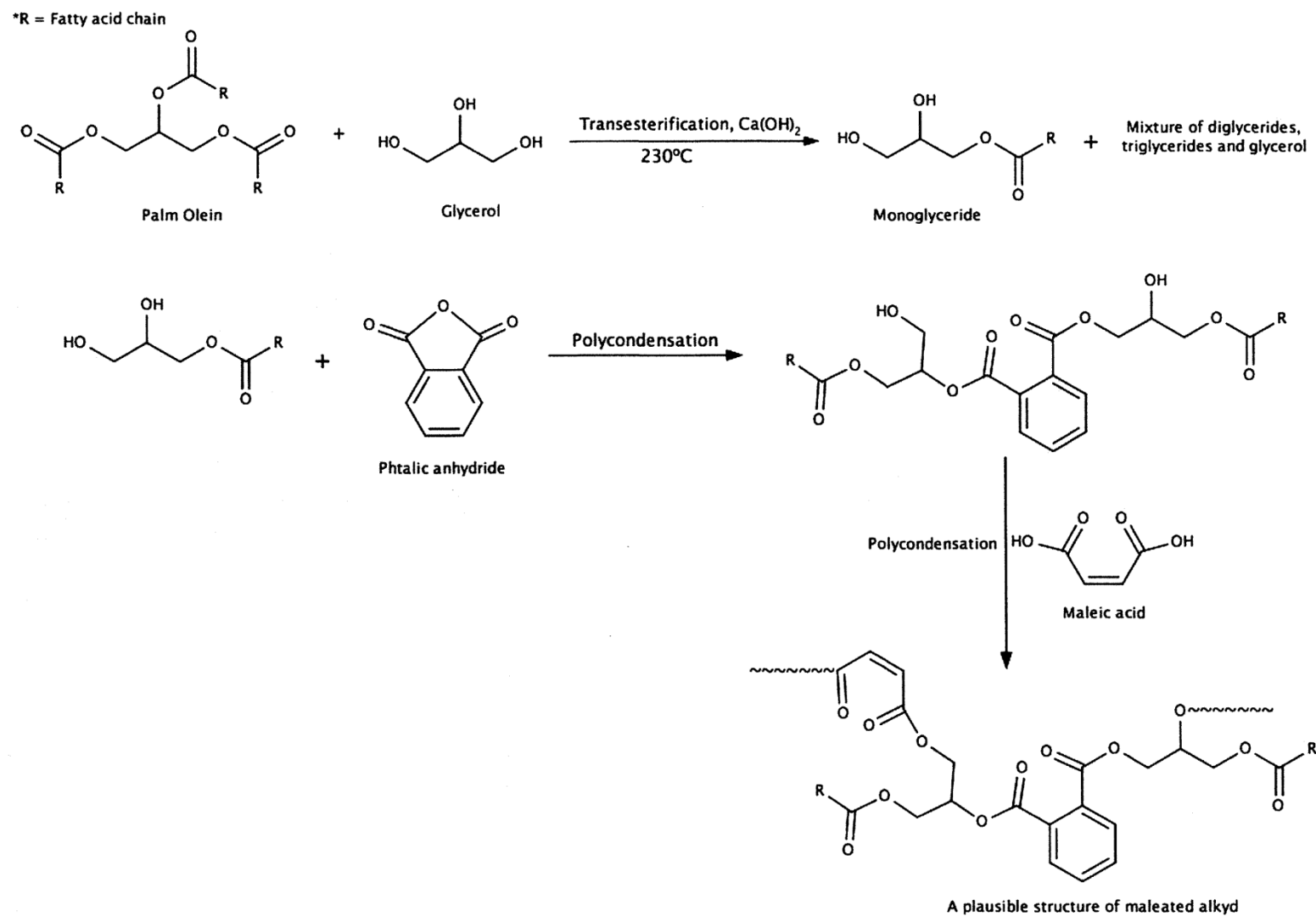


Figure 4.5: Plausible synthesis route of the maleated alkyd

4.2.4 Thermal analysis

For TGA analysis, in Figure 4.6, the TGA thermogram shows the onset of degradation of the alkyd was at 179°C while the 1st TGA derivative curve of the alkyd shows maximum rate of decomposition at 377°C (Ramlan et al., 2017). At 200°C to 450°C, first degradation step happen due to alkyd while the second degradation step at 500°C to 650°C is due to the degradation of secondary product generated from the heating of alkyd.

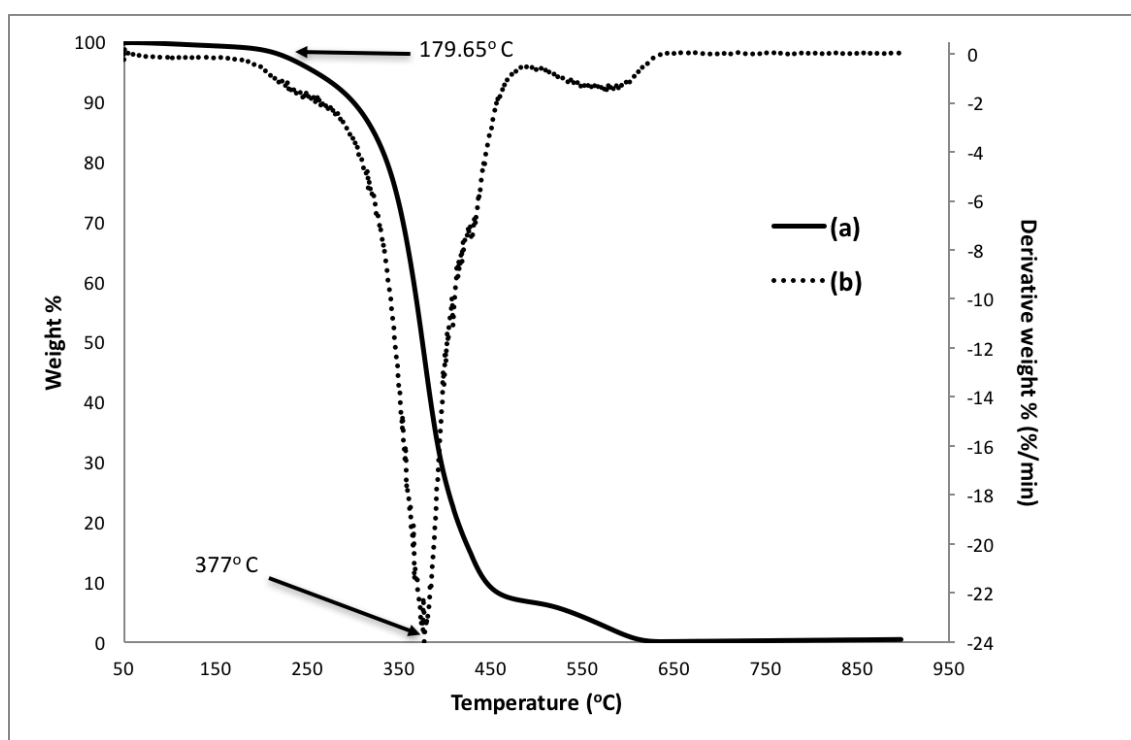


Figure 4.6: (a) TGA thermogram of alkyd and (b) 1st TGA derivative curve (%/min against temperature) of alkyd

4.3 Characterizations of PANI

4.3.1 FTIR spectroscopy

In PANI characterization, the FTIR spectrum of PANI was shown in Figure 4.7. The peaks from $3700 - 3000 \text{ cm}^{-1}$ corresponded to the N-H stretching vibration. The characteristics peaks of conducting PANI are at 1587 and 1488 cm^{-1} , were attributed to quinoid and benzenoid rings stretching vibration mode, respectively. Meanwhile, the appearance of peak at 1297 cm^{-1} was noted as the stretching of C-N^+ in the polaron structure which indicates that the PANI was in its conducting form. The lower region peak at 814 cm^{-1} wavenumber represented the aromatic ring and out-of-plane deformation vibrations (Lim et al., 2013; Sambasevam et al., 2015).

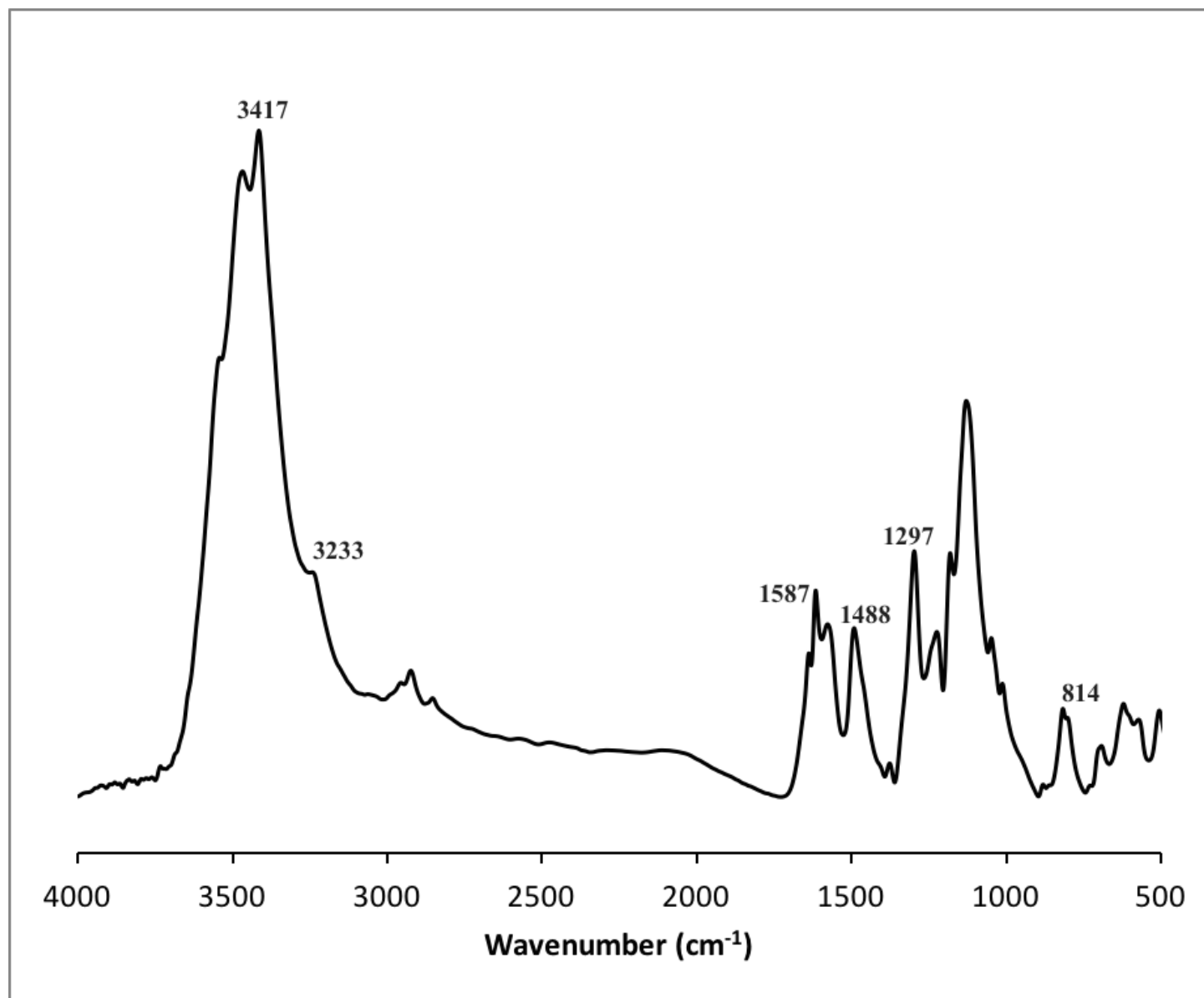


Figure 4.7: FTIR spectrum of PANI

4.3.2 UV-Vis spectroscopy

The UV-Vis spectrum of PANI was shown in Figure 4.8. Usually, PANI will show three characteristic peaks at ~340–350 nm, ~426–433 nm, and ~775–786 nm. The absorption peak at 347 nm was contributed by $\pi-\pi^*$ transition of the benzenoid rings, while the peaks at 428 nm and 755 nm were shown by polaron- π^* and π -polaron transitions respectively (Xia & Wang, 2001). Furthermore, the doping level and formation of polarons were discussed based on the peaks at ~426–433 nm and ~775–786 nm. As reported by Xia and Wang, the absorbance ratio of ~775–786 nm (π -polaron) to ~340–350 nm ($\pi-\pi^*$ transition) can estimate the doping level, where the high absorbance ratio value indicates the high level of doping in the PANI emeraldine salt structure (Xia & Wang, 2001). Based on Figure 4.8, the absorbance obtained from 347 nm was 0.443 while the absorbance at 755 nm was 0.64. The calculated absorbance ratio was 1.447 which was considered high (Sambasevam et al., 2015).

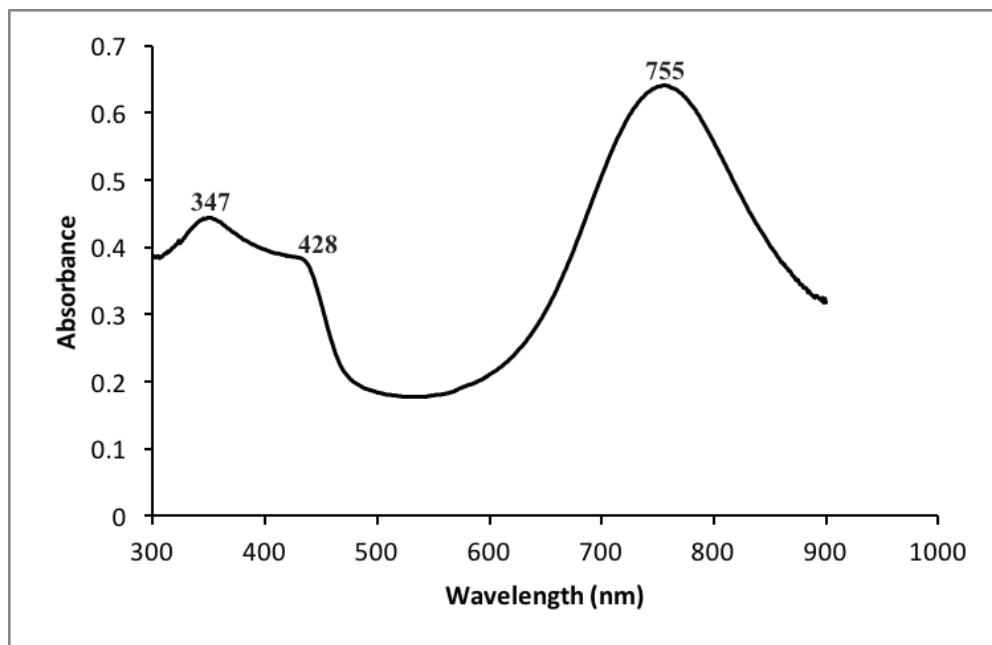


Figure 4.8: UV-Vis spectrum of PANI

4.3.3 Thermal analysis

From TGA analysis, the TGA thermogram of PANI in Figure 4.9 shows three degradation steps. The early stage of degradation up to 105 °C may be attributed to the release of adsorbed water molecules or moisture within the layers. The second stage of degradation can be observed from 105 °C to 230 °C, may be due to the loss of dopant in this case, organic sulfonic acid. The third stage of degradation occurred on 230 °C and above may be attributed to the degradation of polymer backbone (Bansal et al., 2009).

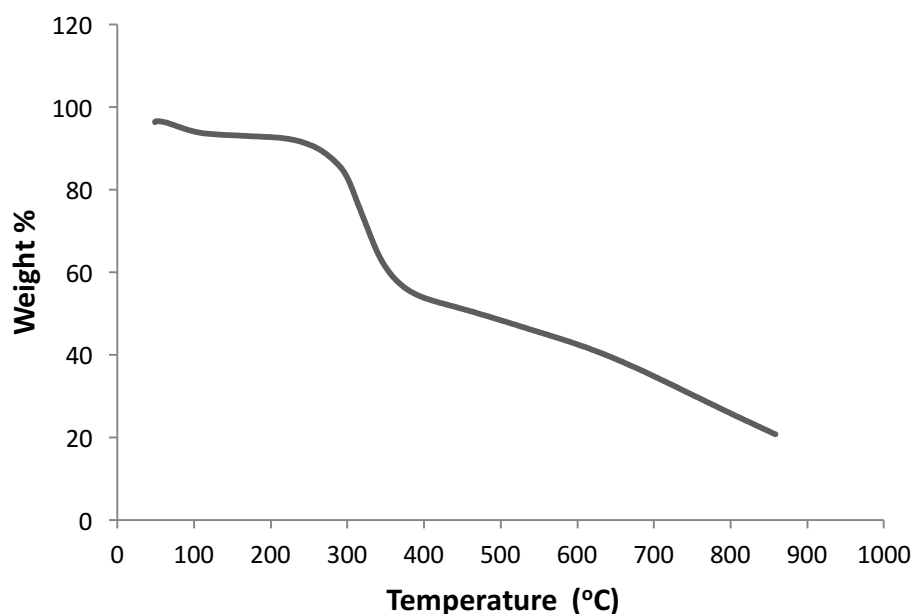


Figure 4.9: TGA thermogram of PANI

4.4 Alkyd/PANI Film Properties

4.4.1 Effect of coating composition (Alkyd:PANI) on film conductivity

Table 4.5 shows the results of the conductivity of alkyd coatings containing different proportions of PANI coated on glass slides. The average conductivity of the neat PANI was 5.989×10^0 S/cm. The coating films started to be conductive with 20% addition of PANI. The drop in the conductivity as compared to neat PANI was expected as the alkyd matrix is non-conductive in nature. Nevertheless, the conductivity of the alkyd/PANI recorded is still considered very high, in the range of 10^{-1} to 10^{-3} S/cm (Ramlan et al., 2017). The addition of m-cresol has contributed to the increased in the conductivity of the film through secondary doping (Pereira da Silva et al., 1999; Valenciano et al., 2000).

Table 4.5: Conductivity of coating mixtures contain different ratios of alkyd and PANI

Coating Mixture	Alkyd : PANI powder ratio	Average thickness on glass slide (μm)	Conductivity (S/cm)
A	10 : 0	20	-
B	9 : 1	19	-
C	8.5 : 1.5	18	-
D	8 : 2	21	2.756×10^{-3}
E	7 : 3	22	3.735×10^{-2}
F	6 : 4	16	1.467×10^{-1}

4.4.2 UV-Vis spectroscopy

Figure 4.10 shows the UV-Vis spectra of alkyd and alkyd/PANI coatings. For Coating A that contain alkyd only, there was only one absorption peak around 300 nm. For coatings D, E and F that contain mixtures of alkyd and PANI, there were another three absorption peaks around 340 nm, 440 nm and 780 nm showing PANI characteristic peaks other than peak form alkyd around 300 nm. These three characteristic peaks have different absorbance for each coating based on the level of doping as discussed earlier in section 4.3.2. Table 4.6 shows the assignments of UV-Vis absorption peaks for coatings D, E and F. The results denote that Coating F keep the highest degree of doping extension, followed by Coating E and Coating D. This result consistent with the conductivity of coatings determined before. The absorbance ratios were increasing with increasing percentage of PANI in coatings; increasing conductivity. This trend was expected since the higher the absorbance ratio value, the higher the doping level in the emeraldine salt structure of PANI (Xia & Wang, 2001; Sambasevam et al., 2015).

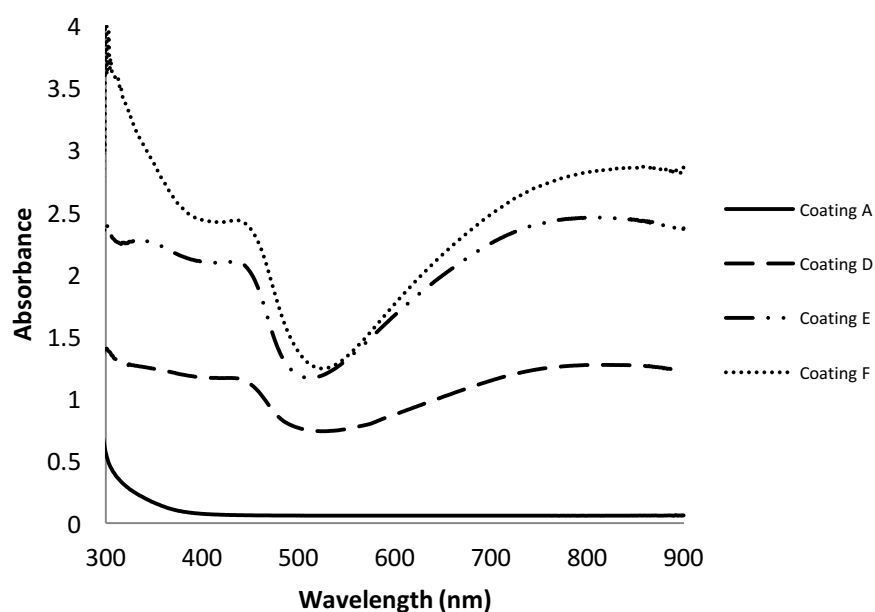


Figure 4.10: UV-Vis spectra of alkyd & alkyd/PANI coatings

Table 4.6: UV-Vis absorption peaks assignments for alkyd/PANI coatings

Coating	$\pi-\pi^*$ transition (nm)	Absorbance	π -polaron transition (nm)	Absorbance	Absorbance ratio $A_{775-786}/A_{340-350}$
D	345	1.248	783	1.265	1.0136
E	341	2.270	783	2.446	1.0775
F	388	2.475	781	2.791	1.1277

4.4.3 Film properties

The physicochemical properties of UV-cured coatings are presented in Table 4.7. The pencil hardness of the coatings did not deviate much with most of the coatings in the range of pencil grade 2B to 4B. The slight decrease in the pencil hardness grade of the coating containing PANI was not unexpected as the extent of crosslinking in the coating decreased when the ratio of PANI : (MMA+alkyd) increased. Alkyd and MMA provided most of the active sites for crosslinking in the coating. The film adhesion of the coating recorded a grade of 5B to 3B, where the addition of PANI led to a slight reduction in the film adhesion. However, the film adhesion is considered reasonably good as the % of film removed was only in the range of 5 to 15 % area lattice (Ramlan et al., 2017).

Being an oil-based coating, the water resistances of the coatings were generally good. The coatings were not severely affected from the 24 hr immersion in distilled water. The whitening which was present in Coating A and D disappeared in less than 2h of drying at room temperature. Coating E and F showed excellent resistance towards the water and were not visibly affected (Ramlan et al., 2017).

In the alkali resistance test, coating A dissolved completely in alkali solution which was expected as the ester linkages in the resin are feeble towards alkali hydrolysis. After the test, all coatings that consisted of PANI turned from green color to

blue since the emeraldine salt of PANI was converted to emeraldine base. Coating E and F showed improve resistance towards diluted alkali since there were no detachments observed even, after 5 min of immersion (Ramlan et al., 2017).

Another two chemical resistance tests were conducted both in acid (0.1M HCl) and saltwater (5% NaCl). All tested coating films showed excellent resistance towards acid solution and saltwater as no detachment was observed (Ramlan et al., 2017).

Table 4.6: Physicochemical properties of UV-cured coatings

Coating	Pencil Hardness	Film Adhesion		Water resistance ^a	Alkali resistance (min) ^b	Acid resistance ^c	Saltwater resistance ^c
		Grade	%				
A	2B	5B	0	II	1	✓	✓
D	4B	4B	2	II	2.5	✓	✓
E	4B	4B	4	I	>5	✓	✓
F	4B	3B	10	I	>5	✓	✓

^a Coating conditions after 24h of immersion in water (I = not visibly affected; II = whitening present but disappear after 2h of drying in room temperature)

^b Duration of immersion (min) in 30 g/L NaOH before apparent film defects (flaked off)

^c Coating conditions after 1h of immersion in solutions at 80°C (✓ = not visibly affected)

4.4.4 Thermal Analysis

The thermal stability of alkyd and alkyd/PANI coatings was investigated using TGA. The results from the thermogravimetric analysis were applied to the Kissinger equation to determine the activation energy of decomposition, E_d of the coating (Ang et al., 2016; Zabihi & Khodabandeh, 2013; Zhang et al., 2015). Thermal degradation kinetic parameters were investigated using this method, and the Kissinger equation is expressed as:

$$-\ln \left(\frac{q}{T_p^2} \right) = \frac{E_d}{RT_p} - \ln \left(\frac{AR}{E_d} \right) \quad (\text{Eqn. 4.1})$$

Where; q = heating rate

T_p = peak temperature at which maximum decomposition occurs

E_d = activation energy of decomposition

A = pre-exponential factor

R = gas constant

Three different heating rates of 10, 20 and 30 °C/min were conducted on coatings A, D, E and F using TGA. From derivative TGA thermograms, the peak temperature (in Kelvin) where the first maximum decomposition occurred was taken as T_p . The activation energy of decomposition, E_d values for coatings A, D, E, and F was calculated based on the gradients from the plot of $-\ln (q/T_p^2)$ against $1000/T_p$ (Ang et al., 2016) were shown in Table 4.8. The results showed that there was a slight reduction in the E_d of the PANI/Alkyd coating as compared to neat alkyd coating. Presumably, the reduction in the extent of crosslinking in the PANI/Alkyd coatings owed to the relatively less C=C from reduced amount of alkyd in the coating that could have led to the observed trend. The result is consistent with the results of pencil hardness test

(Ramlan et al., 2017). Besides, PANI was reported to have limited stability at 100 °C to 200 °C as discussed in section 4.3.3.

Table 4.7: E_d of coatings based on Kissinger equation

Coating	T_{p10}/K	T_{p20}/K	T_{p30}/K	$E_d/kJ\ mol^{-1}$
A(control)	527.8	536.9	545.7	138.1
D	623.9	637.0	638.4	96.6
E	579.0	600.9	607.7	96.9
F	605.9	626.0	619.6	98.6

* T_{p10} indicates maximum decomposition temperature at heating rate 10 K/min

4.4.5 Effect of UV curing time on film conductivity and FTIR analyses

The conductivity of coating F with different UV curing times is shown in Table 4.9. The results show that there was a slight reduction in the conductivity of the coatings after it was exposed to the UV irradiation. It is worth to mention that the reduction of conductivity was very minimal as the final and initial conductivity were still well within the range of 10^{-1} S/cm. The results obtained were similar to other reported studies (Kawata et al., 2013; Virji et al., 2004). Kawata and companions recorded the decreasing of conductivity of PANI/TiO₂/alkyd from 7.290×10^1 S/cm to 9.029×10^0 S/cm with increasing UV curing time. The slight reduction observed in this work was attributed to the decrease in the relative amount of benzenoid form of PANI that contributed to the delocalization of electron for conductivity purposes.

The FTIR analyses on the films were conducted to study the plausible structural changes of the PANI that affected the conductivity. Figure 4.11 shows the FTIR spectra of the same coating irradiated with UV light for different intervals of time. The changes observed in the spectra agreed that there were some structural changes to the PANI, where some of its benzenoid ($\sim 1465\ cm^{-1}$) forms were converted to quinoid upon UV

irradiation. The latter was expected to participate in the crosslinking reaction with the coating components such as the alkyd resin and MMA. Such interactions between PANI and coating components are important to maintain product stability and lead to improvement in properties such as film adhesion and mechanical strength (Kawata et al., 2013).

The neat PANI film was also prepared to serve as a control. The film was irradiated with UV light for up to 120 s while the conductivity of the film recorded remained approximately constant throughout the test. The results obtained supported the above observation and showed that the alkyd resins are needed for the drop in conductivity to be observed. Alkyd and MMA provide reactive C=C that could undergo crosslinking with each other and with the unsaturation in the quinoid moiety of PANI. This is a good indication that suggests that the UV irradiation could have aided with the integration of PANI and alkyd resin in the coatings (Ramlan et al., 2017). Although there is reduction in conductivity, the final conductivity of the coating is still reasonably high, well around $10^{-1} \text{ S cm}^{-1}$.

Table 4.8: Conductivity of coating F with different UV curing times

UV curing time (s)	Average thickness on glass slide (μm)	Conductivity ($\times 10^{-1} \text{ S/cm}$)
0	7	5.752
30	7	3.167
60	7	2.780
90	7	1.490
120	7	1.135

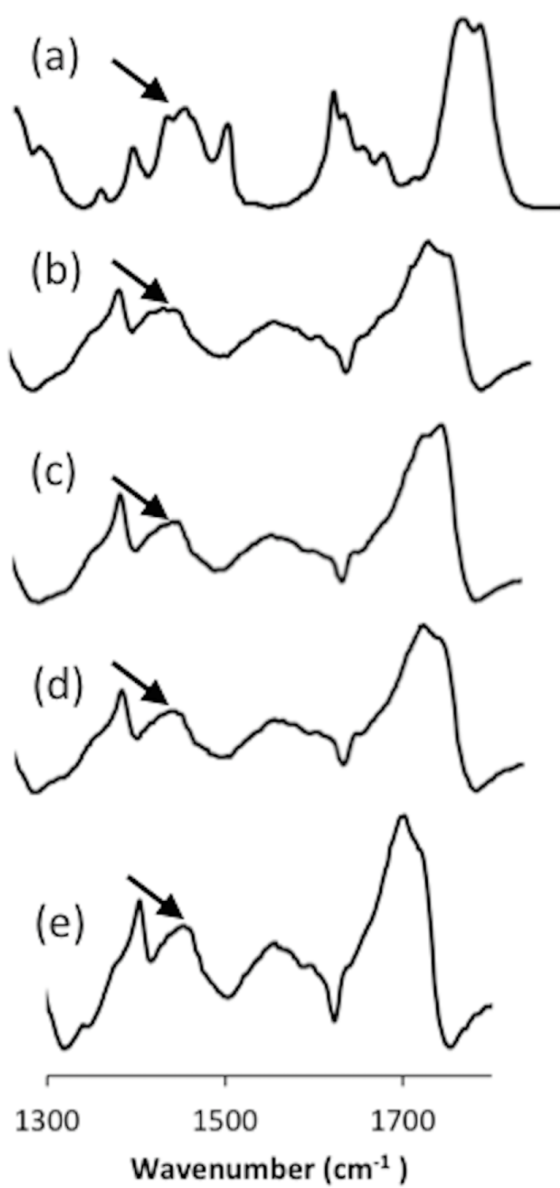


Figure 4.11: Overlay of FTIR spectra of coating F with different UV curing times; (a) 0s, (b) 30s, (c) 60s, (d) 90s and (e) 120s

4.5 Surface and electrochemical study

4.5.1 Field-emission scanning electron microscopy analysis (FESEM)

Figure 4.12(a) shows the FESEM images of Coating K which was a control coating that contain alkyd only. Based on the images captured, the morphology of coating is clean and smooth with no particles. Figure 4.12(b) shows the FESEM images of Coating L which contain alkyd and 0.5% PANI. This coating shows a good dispersion of PANI powder with no agglomeration in the surface coating.

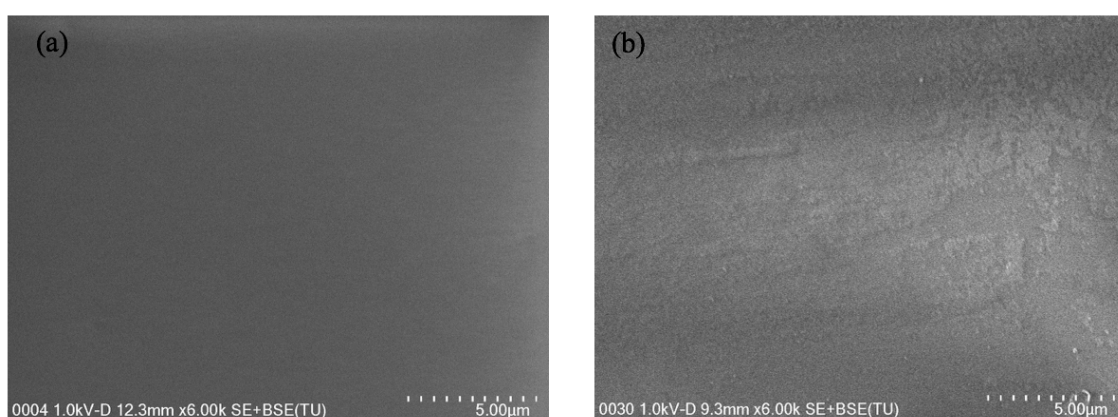


Figure 4.12: FESEM images of (a) Coating K and (b) Coating L

4.5.2 Open circuit potentials analysis

Figure 4.13 shows the decrement value of OCP by coating K (control alkyd/MMA) while the OCP of coating L (0.5% PANI) and M (1% PANI) started to shift upwards toward the positive value throughout 1-30 days of immersion in 3.5% NaCl. The presence of PANI in Coating L and Coating M could favor the oxidation of ferrous ions to stable passive iron oxide film at the pin hole region thus the OCP value increasing and produces a more stable coating against corrosion (Sathiyanarayanan et al., 2005).

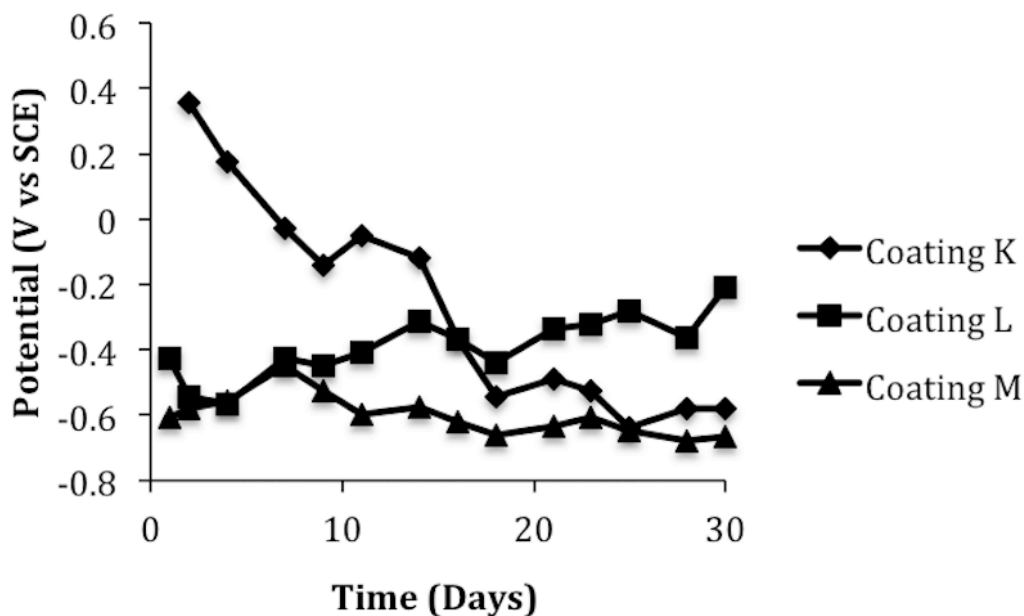


Figure 4.13: OCP variations of coated steel K, L and M during 30 days immersion in 3.5% NaCl

4.5.3 EIS analysis

Figure 4.14 shows the Nyquist plots of impedance spectra in various immersion times for coatings K, L, and M coated on mild steel in 3.5% NaCl solution. As expected, based on the semicircle observed, the impedance values decreased in all coatings after a long exposure time. The behavior of the fitted Nyquist and Bode plots were simulated with one time constant equivalent circuit and all the impedance parameters such as; coating resistance (R_c), double layer capacitance (C_{dl}), solution resistance (R_s), charge transfer resistance (R_{ct}), coating capacitance (C_c) and constant phase element (Q) of the prepared coatings were recorded in Table 4.10. From the coating resistance value, R_c ($\Omega \text{ cm}^2$) at 25th days (Figure 4.12), it can be observed that coatings L and M have high R_c value compared to coating K (control) (Ramlan et al., 2017). The protective nature of PANI coating contributed to the high resistance values, R_c and low capacitance value, Q_c and may be due to continuous charge transfer reaction that occurred at the metal-coating interface. The impedance values of all coatings were

found to be lower with a decrease in R_c and increase in Q_c due to the ingress of chloride ions and water (Rout et al., 2003; Sathiyarayanan et al., 2005).

Table 4.9: Impedance parameters of coatings K, L and M coated on mild steel in 3.5% NaCl solution

Coating K			
Time (days)	$R_c (\Omega \text{ cm}^2)$	$Q_c (\text{F cm}^{-2})$	n
1	203.7×10^3	0.5668×10^{-7}	0.6512
4	105.5×10^3	0.156×10^{-5}	0.4131
14	8.47×10^3	0.5887×10^{-6}	0.516
25	1.864×10^3	0.3682×10^{-6}	0.6239
30	3.94×10^3	0.6964×10^{-3}	0.4384
Coating L			
Time (days)	$R_c (\Omega \text{ cm}^2)$	$Q_c (\text{F cm}^{-2})$	n
1	0.741×10^6	0.4691×10^{-8}	0.8087
4	260.9×10^3	0.1119×10^{-7}	0.7424
14	14.52×10^3	0.2754×10^{-5}	0.6235
25	15.33×10^3	0.2902×10^{-6}	0.5814
30	13.59×10^3	0.3919×10^{-6}	0.5595
Coating M			
Time (days)	$R_c (\Omega \text{ cm}^2)$	$Q_c (\text{F cm}^{-2})$	n
1	35.3×10^3	0.3956×10^{-5}	0.3787
4	63.6×10^3	0.1024×10^{-5}	0.5320
14	2.393×10^3	0.8922×10^{-6}	0.6967
25	14.71×10^3	0.2253×10^{-3}	0.5642
30	3.34×10^3	-	-

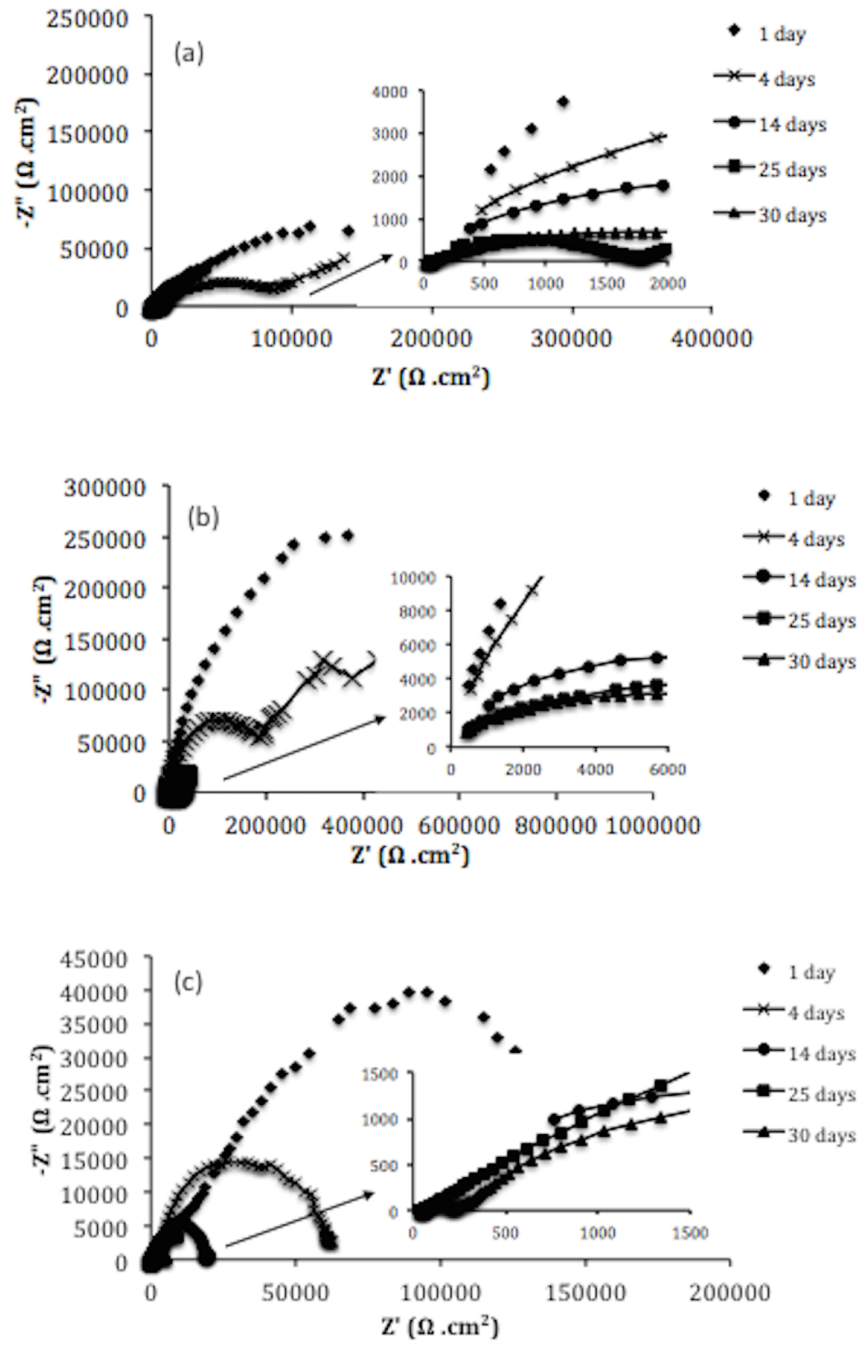


Figure 4.14: Nyquist plots of impedance spectra in various immersion times for (a) Coating K, (b) Coating L and (c) Coating M coated on mild steel in 3.5% NaCl solution

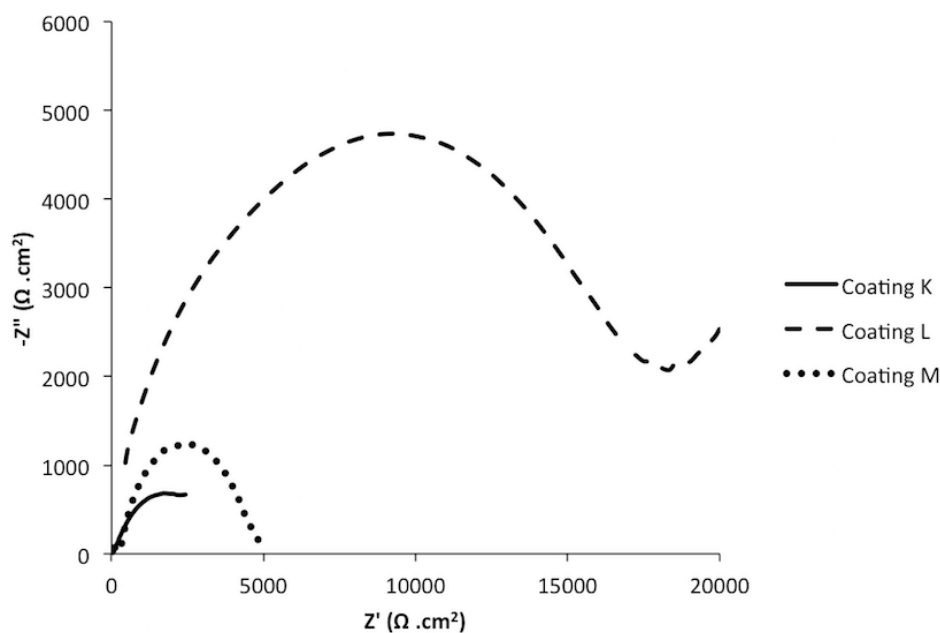


Figure 4.15: Nyquist plots of impedance spectra after 25 days immersion of Coating K, L and M coated on mild steel in 3.5% NaCl solution

4.5.4 Tafel polarization measurements

Based on Table 4.11 and Figure 4.16, it can be seen that coating L (0.5% PANI) had lower corrosion rate followed by coating M (1% PANI) and coating K (control) because of the passive behavior of the PANI coated steel (Rout et al., 2003). The extrapolation of Tafel region of polarization curve of coating L shows the smallest current density (6.129×10^{-7} A) and more noble potential (-445mV) compared to other coatings (Ramlan et al., 2017). Based on the visual observation on the coatings after 30 days being immersed in 3.5% NaCl as shown in Figure 4.17, it can be concluded that coating K is the most affected coating by corrosion product (rust) whereas coating L has oxide layer on the surface of coating followed by coating M. Coating L with addition of 0.5% PANI has achieved optimum percentage of PANI as additive in coating to exhibit its anti-corrosion properties.

The excellent electrical conductivity and electrochemical property of the coating showed that the product has many potential applications especially in the development of sensors and could be potentially simulated into intelligence technology (Alippi, 2016; Zhang et al., 2016).

Table 4.10: Data from Tafel Plot analysis

Coating	I_{corr} (Acm^{-2})	β_c (V/dec)	β_a (V/dec)	R_p ($\text{k}\Omega$ cm^2)	E_{corr} (V)	Corrosion rate (mm/y)
K	4.545×10^{-5}	0.252	0.572	0.4379	-1.083	5.304×10^{-3}
L	1.951×10^{-7}	0.176	0.209	26.07	-0.445	2.277×10^{-5}
M	5.795×10^{-6}	0.173	0.204	0.846	-0.815	6.763×10^{-4}

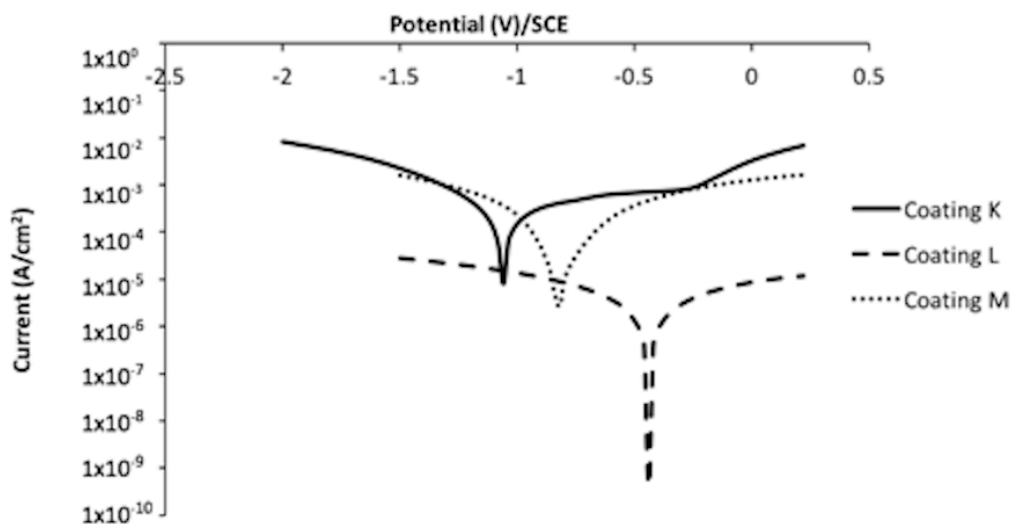


Figure 4.16: Tafel Plot for coating K (Alkyd), coating L (0.50% PANI) and coating M (1% PANI)

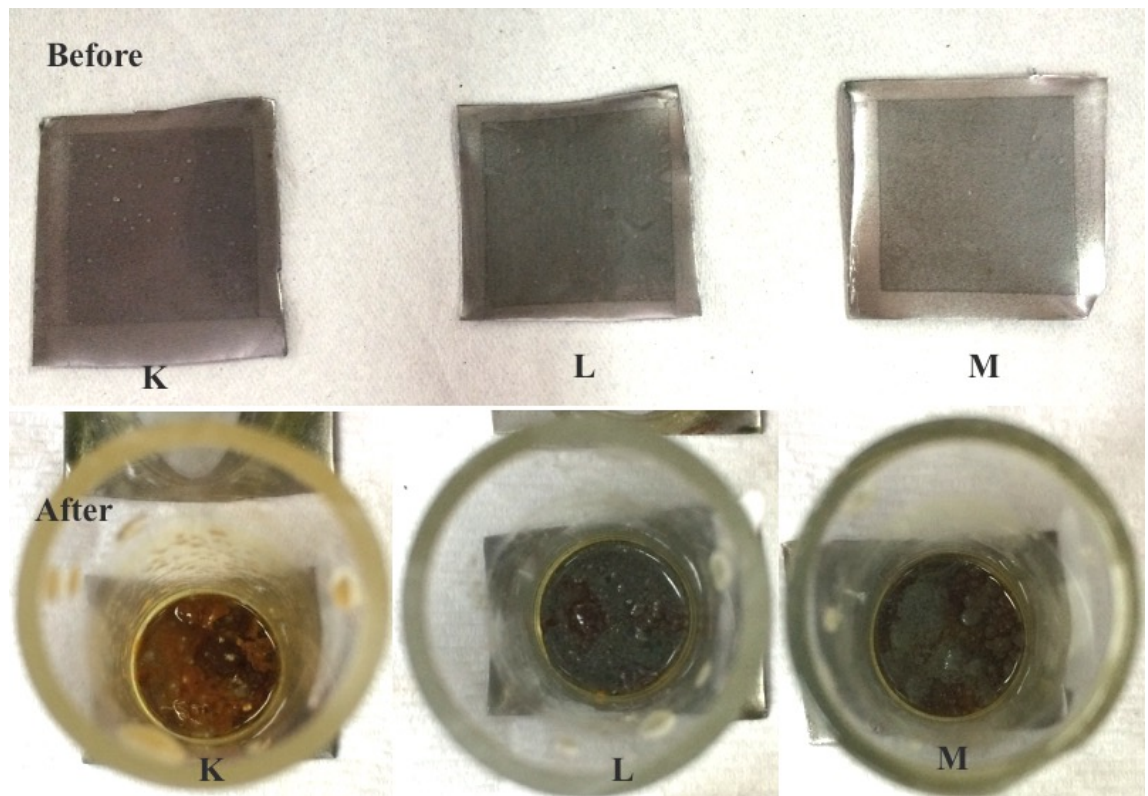


Figure 4.17: Coated mild steels for coating K, L and M before and after immersed in 3.5% NaCl for 30 days

CHAPTER 5: CONCLUSIONS AND SUGGESTION FOR FURTHER RESEARCH

5.1 Conclusions

Unsaturated alkyd was successfully synthesized using palm oil as the source of fatty acids with contribution of diacids; phthalic anhydride and maleic acid to increase the unsaturation for radiation curable purpose. This alkyd was characterized using FTIR and ^1H -NMR spectroscopy and then compared with palm olein. The presence of peak at 1647 cm^{-1} wavenumber and 6.92 ppm for FTIR and ^1H -NMR spectroscopy of this alkyd respectively indicates the unsaturated part of maleic acid in the system.

Polyaniline (PANI) was characterized by FTIR and UV-Vis spectroscopy to confirm it is in conducting form which was emeraldine salt. The stretching of quinoid and benzenoid rings presented in FTIR spectroscopy and three characteristics peaks observed in UV-Vis spectrum indicate the conducting form of PANI.

The physical and anti-corrosive properties of UV-cured alkyd/polyaniline coatings on steel were investigated. The mechanical properties of alkyd coating did not change much with the addition of polyaniline. At lower PANI loading, the coating has shown improved corrosion resistance properties.

Here, an environmentally friendly UV-curable palm oil-based coating was made electrically active by incorporating PANI into the system. There were evidences of strong interaction between alkyd and polyaniline from the FTIR analyses and conductivity studies. The conversion of benzenoid to a quinoid form of PANI followed by a slight reduction in conductivity of the Alkyd/PANI coating during UV irradiation

suggested the occurrence of crosslinking between the two components which are crucial to produce a stable and homogeneous coating film.

5.2 Suggestion for further research

In future, it would be more interesting if more alkyds are synthesized by varying the formulation with different source of unsaturation and produce alkyds with different acid numbers. By that, more comparison on film properties, homogeneity of coating mixtures of alkyd/PANI and its UV-curability can be determined.

Besides, it would be rather interesting to combine the alkyd with other conductive polymers such as polypyrrole and polythiophene in order to investigate the performance of conductivity level and anti-corrosion study.

In this project, the photoinitiator used is restricted by one type only which was benzophenone. It would be an interesting objective to use different kind of photoinitiator to compare the UV-curability and time taken to cure with resulting a good film properties of coating.

REFERENCES

- Aigbodion, A. I., Okieimen, F. E., Obazee, E. O., & Bakare, I. O. (2003). Utilisation of maleinized rubber seed oil and its alkyd resin as binders in water-borne coatings. *Progress in Organic Coatings*, 46(1), 28-31.
- Alam, J., Riaz, U., & Ahmad, S. (2009). High performance corrosion resistant polyaniline/alkyd ecofriendly coatings. *Current Applied Physics*, 9(1), 80-86.
- Alamer, F. A. (2017). A simple method for fabricating highly electrically conductive cotton fabric without metals or nanoparticles, using PEDOT:PSS. *Journal of Alloys and Compounds*, 702, 266-273.
- Alippi, C. (2016). A unique timely moment for embedding intelligence in applications. *CAAI Transactions on Intelligence Technology*, 1(1), 1-3.
- Amberg, M., Vandenbossche, M., & Hegemann, D. (2018). Controlled Ag release from electrically conductive coating systems. *Surface and Coatings Technology*, 336, 29-33.
- Ang, D. T. C. (2015). Effect of reactive diluent on physicochemical and thermal properties of UV-curable alkyd coatings. *Journal of Coatings Technology and Research*, 1-8.
- Ang, D. T. C., Khong, Y. K., & Gan, S. N. (2016). Palm oil-based compound as environmentally friendly plasticizer for poly(vinyl chloride). *Journal of Vinyl and Additive Technology*, 22(1), 80-87.
- Ang, D. T. C., & Gan, S. N. (2012). Development of palm oil-based alkyds as UV curable coatings. *Pigment & Resin Technology*, 41(5), 302-310.
- Ang, D. T. C., & Gan, S. N. (2012). Novel approach to convert non-self drying palm stearin alkyds into environmental friendly UV curable resins. *Progress in Organic Coatings*, 73(4), 409-414.
- Assanvo, E. F., Gogoi, P., Dolui, S. K., & Baruah, S. D. (2015). Synthesis, characterization, and performance characteristics of alkyd resins based on Ricinodendron heudelotii oil and their blending with epoxy resins. *Industrial Crops and Products*, 65(Supplement C), 293-302.

- Awuzie, C. I. (2017). Conducting Polymers. *Materials Today: Proceedings*, 4(4, Part E), 5721-5726.
- Aydin, S., Akçay, H., Özkan, E., Güner, F. S., & Erciyes, A. T. (2004). The effects of anhydride type and amount on viscosity and film properties of alkyd resin. *Progress in Organic Coatings*, 51(4), 273-279.
- Azimi, A. R. N., Yahya, R., & Gan, S.-N. (2013). Improving coating characteristics of palm stearin alkyd by modification with ketone resin. *Progress in Organic Coatings*, 76(4), 712-719.
- Bandeira, R. M., van Drunen, J., Tremiliosi-Filho, G., dos Santos, J. R., & de Matos, J. M. E. (2017). Polyaniline/polyvinyl chloride blended coatings for the corrosion protection of carbon steel. *Progress in Organic Coatings*, 106(Supplement C), 50-59.
- Bansal, V., Bhandari, H., Bansal, M. C., & Dhawan, S. K. (2009). Electrical and Optical behaviour of poly(aniline-co-8-anilino-1-naphthalene sulphonic acid) – A material for ESD applications. *Indian Journal of Pure & Applied Physics*, 47, 667-675.
- Bhadra, S., Khastgir, D., Singha, N. K., & Lee, J. H. (2009). Progress in preparation, processing and applications of polyaniline. *Progress in Polymer Science*, 34(8), 783-810.
- Boeva, Z. A., & Sergeyev, V. G. (2014). Polyaniline: Synthesis, properties, and application. *Polymer Science Series C*, 56(1), 144-153.
- Bruen, K., Davidson, K., Sydes, D. F., & Siemens, P. M. (2004). Benefits of UV-curable coatings. *European coatings journal*, 4, 42-56.
- Cadena, F., Irusta, L., & Fernandez-Berridi, M. J. (2013). Performance evaluation of alkyd coatings for corrosion protection in urban and industrial environments. *Progress in Organic Coatings*, 76(9), 1273-1278.
- Chattopadhyay, D. K., Panda, S. S., & Raju, K. V. S. N. (2005). Thermal and mechanical properties of epoxy acrylate/methacrylates UV cured coatings. *Progress in Organic Coatings*, 54(1), 10-19.
- Chen, C., Su, M., Liu, G., & Yang, Z. (2013). Evaluation of economic loss from energy-related environmental pollution: a case study of Beijing. *Frontiers of Earth Science*, 7(3), 320-330.

- Cheng, X., Kumar, V., Yokozeiki, T., Goto, T., Takahashi, T., Koyanagi, J., . . . Wang, R. (2016). Highly conductive graphene oxide/polyaniline hybrid polymer nanocomposites with simultaneously improved mechanical properties. *Composites Part A: Applied Science and Manufacturing*, 82, 100-107.
- Coltevieille, D., Le Méhauté, A., Challioui, C., Mirebeau, P., & Demay, J. N. (1999). Industrial applications of polyaniline. *Synthetic Metals*, 101(1), 703-704.
- da Silva, J. E. P., de Torresi, S. I. C., & Torresi, R. M. (2007). Polyaniline/poly(methylmethacrylate) blends for corrosion protection: The effect of passivating dopants on different metals. *Progress in Organic Coatings*, 58(1), 33-39.
- Davis, J. R. (2000). *Corrosion: Understanding the Basics*: ASM International.
- Decker, C. (1992). Kinetic Analysis and Performance of UV-Curable Coatings. In S. P. Pappas (Ed.), *Radiation Curing: Science and Technology* (pp. 135-179). Boston, MA: Springer US.
- Decker, C., Keller, L., Zahouily, K., & Benfarhi, S. (2005). Synthesis of nanocomposite polymers by UV-radiation curing. *Polymer*, 46(17), 6640-6648.
- del Amo, B., Romagnoli, R., & Vetere, V. F. (1999). Steel Corrosion Protection by Means of Alkyd Paints Pigmented with Calcium Acid Phosphate. *Industrial & Engineering Chemistry Research*, 38(6), 2310-2314.
- Deshpande, P. P., & Sazou, D. (2016). *Corrosion Protection of Metals by Intrinsically Conducting Polymers*. Florida, US: CRC Press.
- Deyab, M. A., & Keera, S. T. (2014). Effect of nano-TiO₂ particles size on the corrosion resistance of alkyd coating. *Materials Chemistry and Physics*, 146(3), 406-411.
- Dhoke, S. K., Khanna, A. S., & Sinha, T. J. M. (2009). "Effect of nano-ZnO particles on the corrosion behavior of alkyd-based waterborne coatings". *Progress in Organic Coatings*, 64(4), 371-382.
- Dong, F., Maganty, S., Meschter, S. J., & Cho, J. (2018). Effects of curing conditions on structural evolution and mechanical properties of UV-curable polyurethane acrylate coatings. *Progress in Organic Coatings*, 114(Supplement C), 58-67.

- Ecco, L. G., Fedel, M., Ahniyaz, A., & Deflorian, F. (2014). Influence of polyaniline and cerium oxide nanoparticles on the corrosion protection properties of alkyd coating. *Progress in Organic Coatings*, 77(12, Part A), 2031-2038.
- Florio, J. J., & Miller, D. J. (2004). *Handbook Of Coating Additives*. Florida, US: Taylor & Francis.
- Giuri, A., Masi, S., Colella, S., Listorti, A., Rizzo, A., Gigli, G., . . . Corcione, C. E. (2016). UV Reduced Graphene Oxide PEDOT:PSS Nanocomposite for Perovskite Solar Cells. *IEEE Transactions on Nanotechnology*, 15(5), 725-730.
- Gonçalves, G. S., Baldissera, A. F., Rodrigues, L. F., Martini, E. M. A., & Ferreira, C. A. (2011). Alkyd coatings containing polyanilines for corrosion protection of mild steel. *Synthetic Metals*, 161(3), 313-323.
- González, S., Mirza Rosca, I. C., & Souto, R. M. (2001). Investigation of the corrosion resistance characteristics of pigments in alkyd coatings on steel. *Progress in Organic Coatings*, 43(4), 282-285.
- Grgur, B. N., Elkais, A. R., Gvozdenović, M. M., Drmanić, S. Ž., Trišović, T. L., & Jugović, B. Z. (2015). Corrosion of mild steel with composite polyaniline coatings using different formulations. *Progress in Organic Coatings*, 79(Supplement C), 17-24.
- Gu, H., Guo, J., Wei, H., Yan, X., Ding, D., Zhang, X., . . . Guo, Z. (2015). Transparent anhydride-cured epoxy nanocomposites reinforced with polyaniline stabilized nanosilica. *Journal of Materials Chemistry C*, 3(31), 8152-8165.
- Gu, H., Guo, J., Zhang, X., He, Q., Huang, Y., Colorado, H. A., . . . Guo, Z. (2013). Giant Magnetoresistive Phosphoric Acid Doped Polyaniline–Silica Nanocomposites. *The Journal of Physical Chemistry C*, 117(12), 6426-6436.
- Guo, J., Guan, L., Wei, H., Khan, M. A., Zhang, X., Li, B., . . . Guo, Z. (2016). Enhanced Negative Magnetoresistance with High Sensitivity of Polyaniline Interfaced with Nanotitania. *Journal of The Electrochemical Society*, 163(8), H664-H671.
- Guo, J., Long, J., Ding, D., Wang, Q., Shan, Y., Umar, A., . . . Guo, Z. (2016). Significantly enhanced mechanical and electrical properties of epoxy

nanocomposites reinforced with low loading of polyaniline nanoparticles. *RSC Advances*, 6(25), 21187-21192.

Hoyle, C. E. (1990). Photocurable Coatings *Radiation Curing of Polymeric Materials* (Vol. 417, pp. 1-16): American Chemical Society.

IHS Markit. (2016). *Chemical Economics Handbook: Alkyd/Polyester Surface Coatings*. Retrieved from <https://ihsmarkit.com/products/alkyd-polyester-surface-chemical-economics-handbook.html>.

İşeri-Çağlar, D., Baştürk, E., Oktay, B., & Kahraman, M. V. (2014). Preparation and evaluation of linseed oil based alkyd paints. *Progress in Organic Coatings*, 77(1), 81-86.

Islam, M. R., Hosen Beg, M. D., & Jamari, S. S. (2014). Alkyd Based Resin from Non-drying Oil. *Procedia Engineering*, 90(Supplement C), 78-88.

Jin, H., Chen, Q., Chen, Z., Hu, Y., & Zhang, J. (2016). Multi-LeapMotion sensor based demonstration for robotic refine tabletop object manipulation task. *CAAI Transactions on Intelligence Technology*, 1(1), 104-113.

Kalendová, A., Sapurina, I., Stejskal, J., & Veselý, D. (2008). Anticorrosion properties of polyaniline-coated pigments in organic coatings. *Corrosion Science*, 50(12), 3549-3560.

Kalendová, A., Veselý, D., Kohl, M., & Stejskal, J. (2015). Anticorrosion efficiency of zinc-filled epoxy coatings containing conducting polymers and pigments. *Progress in Organic Coatings*, 78(Supplement C), 1-20.

Kawata, K., Gan, S. N., Ang, D. T. C., Sambasevam, K. P., Phang, S. W., & Kuramoto, N. (2013). Preparation of polyaniline/TiO₂ nanocomposite film with good adhesion behavior for dye-sensitized solar cell application. *Polymer Composites*, 34(11), 1884-1891.

Khatoon, H., & Ahmad, S. (2017). A review on conducting polymer reinforced polyurethane composites. *Journal of Industrial and Engineering Chemistry*, 53(Supplement C), 1-22.

Kinyanjui, J. M., Wijeratne, N. R., Hanks, J., & Hatchett, D. W. (2006). Chemical and electrochemical synthesis of polyaniline/platinum composites. *Electrochimica Acta*, 51(14), 2825-2835.

- Laco, J. I. I., Villota, F. C., & Mestres, F. L. (2005). Corrosion protection of carbon steel with thermoplastic coatings and alkyd resins containing polyaniline as conductive polymer. *Progress in Organic Coatings*, 52(2), 151-160.
- Ladan, M., Basirun, W. J., Kazi, S. N., & Rahman, F. A. (2017). Corrosion protection of AISI 1018 steel using Co-doped TiO₂/polypyrrole nanocomposites in 3.5% NaCl solution. *Materials Chemistry and Physics*, 192, 361-373.
- Lanson, H. J. (1985). Chemistry and Technology of Alkyd and Saturated Reactive Polyester Resins *Applied Polymer Science* (Vol. 285, pp. 1181-1204): American Chemical Society.
- Lim, K. S., Chiam, Y. S., Phang, S. W., Chong, W. Y., Pua, C. H., Zulkifli, A. Z., . . . Ahmad, H. (2013). A Polyaniline-Coated Integrated Microfiber Resonator for UV Detection. *IEEE Sensors Journal*, 13(5), 2020-2025.
- Liu, H., Dong, M., Huang, W., Gao, J., Dai, K., Guo, J., . . . Guo, Z. (2017). Lightweight conductive graphene/thermoplastic polyurethane foams with ultrahigh compressibility for piezoresistive sensing. *Journal of Materials Chemistry C*, 5(1), 73-83.
- Liu, H., Gao, J., Huang, W., Dai, K., Zheng, G., Liu, C., . . . Guo, Z. (2016). Electrically conductive strain sensing polyurethane nanocomposites with synergistic carbon nanotubes and graphene bifillers. *Nanoscale*, 8(26), 12977-12989.
- Lotha, G. (2016) Alkyd Resin. In *Encyclopedia Britannica*. Retrieved from <https://www.britannica.com/science/alkyd-resin>.
- Malaysian Palm Oil Council, (2012), Malaysia; MPOC.
- Martí, M., Fabregat, G., Azambuja, D. S., Alemán, C., & Armelin, E. (2012). Evaluation of an environmentally friendly anticorrosive pigment for alkyd primer. *Progress in Organic Coatings*, 73(4), 321-329.
- Mills, D., Mabbutt, S., & Bierwagen, G. (2003). Investigation into mechanism of protection of pigmented alkyd coatings using electrochemical and other methods. *Progress in Organic Coatings*, 46(3), 176-181.
- Oil Palm Knowledge Base, (2014). Retrieved from <https://oilpalmblog.wordpress.com/2014/02/03/2-fatty-acid-composition-of-palm-oil-palm-oil-fractions-and-palm-kernel-oil/>

- Park, J.-M., Kong, J.-W., Kim, D.-S., & Lee, J.-R. (2004). Non-destructive damage sensing and cure monitoring of carbon fiber/epoxyacrylate composites with UV and thermal curing using electro-micromechanical techniques. *Composites Science and Technology*, 64(16), 2565-2575.
- Patton, T. C. (1962). *Alkyd Resin Technology: Formulating Techniques and Allied Calculations*. New York, US: Interscience Publishers.
- Pereira da Silva, J. E., Temperini, M. L. A., & Córdoba de Torresi, S. I. (1999). Secondary doping of polyaniline studied by resonance Raman spectroscopy. *Electrochimica Acta*, 44(12), 1887-1891.
- Pitchaimari, G., & Vijayakumar, C. T. (2014). Studies on thermal degradation kinetics of thermal and UV cured N-(4-hydroxy phenyl) maleimide derivatives. *Thermochimica Acta*, 575(Supplement C), 70-80.
- Preeti, Farukh, M., Vasisth, B., Singhal, S., Gaur, L., Verma, V., . . . Dhawan, S. K. (2017). Nanoferrite Embedded in Poly(O-Toluidine) and Polyaniline Matrix for EMI Shielding. In R. Singh & S. Choudhury (Eds.), *Proceeding of International Conference on Intelligent Communication, Control and Devices : ICICCD 2016* (pp. 1087-1093). Singapore: Springer Singapore.
- Pritom, J. B., Vinoy, K. J., Praveen, C. R., & Giridhar, M. (2017). Electromagnetic interference shielding efficiency of MnO₂ nanorod doped polyaniline film. *Materials Research Express*, 4(2), 025013.
- Ramlan, S. N. A., Basirun, W. J., Phang, S. W., & Ang, D. T. C. (2017). Electrically conductive palm oil-based coating with UV curing ability. *Progress in Organic Coatings*, 112(Supplement C), 9-17.
- Riaz, U., Nwaoha, C., & Ashraf, S. M. (2014). Recent advances in corrosion protective composite coatings based on conducting polymers and natural resource derived polymers. *Progress in Organic Coatings*, 77(4), 743-756.
- Rout, T. K., Jha, G., Singh, A. K., Bandyopadhyay, N., & Mohanty, O. N. (2003). Development of conducting polyaniline coating: a novel approach to superior corrosion resistance. *Surface and Coatings Technology*, 167(1), 16-24.
- Sambasevam, K. P., Mohamad, S., & Phang, S. W. (2015). Enhancement of polyaniline properties by different polymerization temperatures in hydrazine detection. *Journal of Applied Polymer Science*, 132(13), 41746(1-8).

- Saravari, O., Phapant, P., & Pimpan, V. (2005). Synthesis of water-reducible acrylic-alkyd resins based on modified palm oil. *Journal of Applied Polymer Science*, 96(4), 1170-1175.
- Sathiyarayanan, S., Muthukrishnan, S., Venkatachari, G., & Trivedi, D. C. (2005). Corrosion protection of steel by polyaniline (PANI) pigmented paint coating. *Progress in Organic Coatings*, 53(4), 297-301.
- Schwalm, R. (2007). Chapter 2 - The UV Curing Process *UV Coatings* (pp. 19-61). Amsterdam: Elsevier.
- Singh, R., & Choudhary, R. B. (2016). Optical absorbance and ohmic behavior of PANI and PANI/ZnO nanocomposites for solar cell application. *Optik - International Journal for Light and Electron Optics*, 127(23), 11398-11405.
- Sørensen, P. A., Kiil, S., Dam-Johansen, K., & Weinell, C. E. (2009). Anticorrosive coatings: a review. *Journal of Coatings Technology and Research*, 6(2), 135-176.
- Spasojevic, P. M., Panic, V. V., Dzunuzovic, J. V., Marinkovic, A. D., Woortman, A. J. J., Loos, K., & Popovic, I. G. (2015). High performance alkyd resins synthesized from postconsumer PET bottles. *RSC Advances*, 5(76), 62273-62283.
- Teo, S. Y., Lee, S. Y., Coombes, A., Rathbone, M. J., & Gan, S. N. (2016). Synthesis and characterization of novel biocompatible palm oil-based alkyds. *European Journal of Lipid Science and Technology*, 118(8), 1193-1201.
- Thanamongkollit, N., Miller, K. R., & Soucek, M. D. (2012). Synthesis of UV-curable tung oil and UV-curable tung oil based alkyd. *Progress in Organic Coatings*, 73(4), 425-434.
- Tiwari, A., Galanis, A., & Soucek, M. D. (2016). *Biobased and Environmentally Benign Coatings*: Wiley.
- Twite, R. L., & Bierwagen, G. P. (1998). Review of alternatives to chromate for corrosion protection of aluminum aerospace alloys. *Progress in Organic Coatings*, 33(2), 91-100.

- Uzoh, C. F., Obodo, N. J., & Onukwuli, O. D. (2016). Exploring the effect of styrene and anhydride ratio on the coating properties of non-drying vegetable oil based alkyd resin. *Journal of King Saud University - Engineering Sciences*.
- Valenciano, G. R., Job, A. E., & Mattoso, L. H. C. (2000). Improved conductivity of films of ultra high molecular weight polyethylene and polyaniline blends prepared from an m-cresol/decaline mixture. *Polymer*, 41(12), 4757-4760.
- Vickers, M. (2017). *In Search of Toxic Silicon Valley: The Subterranean Poisoning From High Technology Manufacturing*. Washington, US: Marquis Publishing.
- Virji, S., Huang, J., Kaner, R. B., & Weiller, B. H. (2004). Polyaniline Nanofiber Gas Sensors: Examination of Response Mechanisms. *Nano Letters*, 4(3), 491-496.
- Visakh, P. M., Pina, C. D., & Falletta, E. (2017). *Polyaniline Blends, Composites, and Nanocomposites*. Netherlands: Elsevier Science.
- Wei, H., Ding, D., Wei, S., & Guo, Z. (2013). Anticorrosive conductive polyurethane multiwalled carbon nanotube nanocomposites. *Journal of Materials Chemistry A*, 1(36), 10805-10813.
- Wei, H., Wang, Y., Guo, J., Shen, N. Z., Jiang, D., Zhang, X., . . . Guo, Z. (2015). Advanced micro/nanocapsules for self-healing smart anticorrosion coatings. *Journal of Materials Chemistry A*, 3(2), 469-480.
- Elvers, B. (Ed.). (2016). *Ullmann's Polymers and Plastics, 4 Volume Set: Products and Processes*. Germany: Wiley-VCH.
- Wissling, P. (2006). *Metallic Effect Pigments: Fundamentals and Applications*. Germany: Vincentz Network.
- Wu, L., & Baghdachi, J. (2015). *Functional Polymer Coatings: Principles, Methods, and Applications*. New Jersey, US: Wiley.
- Wutticharoenwong, K., Dzikowski, J., & Soucek, M. D. (2012). Tung based reactive diluents for alkyd systems: Film properties. *Progress in Organic Coatings*, 73(4), 283-290.
- Xia, H., & Wang, Q. (2001). Synthesis and Characterization of Conductive Polyaniline Nanoparticles Through Ultrasonic Assisted Inverse Microemulsion Polymerization. *Journal of Nanoparticle Research*, 3(5), 399-409.

- Yang, C., Wei, H., Guan, L., Guo, J., Wang, Y., Yan, X., . . . Guo, Z. (2015). Polymer nanocomposites for energy storage, energy saving, and anticorrosion. *Journal of Materials Chemistry A*, 3(29), 14929-14941.
- Yun, Y.-H., Lee, C.-M., Kim, Y.-S., & Yoon, S.-D. (2017). Preparation of chitosan/polyvinyl alcohol blended films containing sulfosuccinic acid as the crosslinking agent using UV curing process. *Food Research International*, 100(Part 1), 377-386.
- Zabihi, O., & Khodabandeh, A. (2013). Understanding of thermal/thermo-oxidative degradation kinetics of polythiophene nanoparticles. *Journal of Thermal Analysis and Calorimetry*, 112(3), 1507-1513.
- Zhang, S., Wang, S., Huang, Z., Li, Y., & Tan, Z. (2015). A kinetic analysis of thermal decomposition of polyaniline and its composites with rare earth oxides. *Journal of Thermal Analysis and Calorimetry*, 119(3), 1853-1860.
- Zhang, X., Gao, H., Guo, M., Li, G., Liu, Y., & Li, D. (2016). A study on key technologies of unmanned driving. *CAAI Transactions on Intelligence Technology*, 1(1), 4-13.
- Zhang, X., He, Q., Gu, H., Colorado, H. A., Wei, S., & Guo, Z. (2013). Flame-Retardant Electrical Conductive Nanopolymers Based on Bisphenol F Epoxy Resin Reinforced with Nano Polyanilines. *ACS Applied Materials & Interfaces*, 5(3), 898-910.
- Zhang, X., He, Q., Gu, H., Wei, S., & Guo, Z. (2013). Polyaniline stabilized barium titanate nanoparticles reinforced epoxy nanocomposites with high dielectric permittivity and reduced flammability. *Journal of Materials Chemistry C*, 1(16), 2886-2899.
- Zhao, Y., Xing, C., Zhang, Z., & Yu, L. (2017). Superhydrophobic polyaniline/polystyrene micro/nanostructures as anticorrosion coatings. *Reactive and Functional Polymers*, 119(Supplement C), 95-104.
- Zhu, J., Gu, H., Luo, Z., Haldolaarachige, N., Young, D. P., Wei, S., & Guo, Z. (2012). Carbon nanostructure-derived polyaniline metacomposites: electrical, dielectric, and giant magnetoresistive properties. *Langmuir*, 28(27), 10246-10255.

LIST OF PUBLICATIONS AND PAPERS PRESENTED

ISI Publication

Ramlan, S. N. A., Basirun, W. J., Phang, S. W., & Ang, D. T. C. (2017). Electrically conductive palm oil-based coating with UV curing ability. *Progress in Organic Coatings*, 112(Supplement C), 9-17.

Conference and presentation

Ramlan, S. N. A., Basirun, W. J., Phang, S. W., & Ang, D. T. C. (2016). Electrically Conductive Coatings Derived from Palm Oil, *International Symposium on Coatings & Corrosion 2016 (ISCC2016)*, 10th International Materials Technology Conference & Exhibition: 16th-19th May 2016, Putra World Trade Center, Kuala Lumpur.